Extended Hubbard model at weak coupling

P.G.J. van Dongen
Institut für Theoretische Physik C, Rheinisch-Westfälische Technische Hochschule (RWTH) Aachen, 52056 Aachen, Germany
(Received 18 March 1994; revised manuscript received 2 May 1994)

The half-filled extended Hubbard model (including nearest-neighbor interaction) is considered in perturbation theory at weak coupling on a d-dimensional hypercubic lattice ($d \gtrsim 3$). It is shown that the *exact* critical temperature and the *exact* order parameter in the weak-coupling limit differ from the corresponding Hartree results by a renormalization factor q of order unity. This renormalization factor q is calculated systematically up to $O(1/d)$ in a $1/d$ expansion. The results depend sensitively on dimension and on the relative strength of the nearest-neighbor interaction. The renormalization factor in $d = 3$, estimated from the $1/d$ expansion, is $q \simeq 0.282$ for the pure Hubbard model, $q \simeq 0.179$ near the spin-density-wave to charge-density-wave transition and $q \simeq 0.830$ in the limit of pure nearest-neighbor interaction.

I. INTRODUCTION

It is well known[1,2] that Hartree-Fock theory, the canonical mean field theory for interacting many-particle systems, is equivalent to self-consistent first-order perturbation theory. As a consequence, Hartree-Fock predictions are asymptotically exact at weak coupling, at least up to *linear* order in the interaction. However, many Hartree-Fock predictions, in particular, those concerning symmetry breaking, involve physical quantities that (at weak coupling) are much smaller than linear in the interaction. For instance, the order parameter and the critical temperature are *exponentially small* as a function of the coupling constant, both in antiferromagnetic Hartree-Fock theory for the Hubbard model[3] and in the BCS theory of superconductivity.[4]

The central question addressed in this paper is, therefore, what is the relevance of Hartree-Fock theory for the low-temperature phase in the weak-coupling limit? In view of the Mermin-Wagner theorem[5] this question is of interest only in higher dimensions ($d \geq 3$) and possibly for the ground state in $d = 2$. To test the quality of Hartree-Fock theory in higher dimensions we consider the *extended Hubbard model*, which is a standard model for electrons on a lattice, interacting through short-range (screened) Coulomb repulsion. For this model we show that although the Hartree-Fock predictions for the low-temperature phase in higher dimensions are *qualitatively* satisfactory, *quantitatively* they can be off by a factor of three to five. A summary of the main results of this paper was previously published as Ref. 6. Here we present the details.

The pure Hubbard model describes itinerant electrons on a lattice, interacting through on-site Coulomb repulsion. Since its introduction in 1963 by Hubbard, Gutzwiller, and Kanamori,[7] the Hubbard model has become a standard model for correlated fermions on a lattice. It has been used to explain various important phenomena in condensed matter physics. Examples are the (Mott-Hubbard) metal-insulator transition,[7,8] the paramagnetic-antiferromagnetic transition,[9,10] ferromagnetism,[11] incommensurate phases,[12] and, most recently, high-T_c superconductors in their normal state.[13,14] However, it has been pointed out already by Hubbard[7] that the Hubbard Hamiltonian as it stands can be derived only under rather drastic assumptions. Many other interaction parameters, some of which may appreciably affect the phase diagram, are simply neglected. The largest of these is the matrix element for nearest-neighbor Coulomb repulsion. The generalization of the Hubbard model that includes also nearest-neighbor interaction is usually referred to as the *extended* Hubbard model.

Accordingly, the Hamiltonian of the extended Hubbard model has the form

$$H = H_t + H_U + H_V + H_\mu \,, \tag{1}$$

where

$$H_t = -\frac{t}{\sqrt{2d}} \sum_{\langle \mathbf{ij} \rangle, \sigma} \left(c^\dagger_{\mathbf{i}\sigma} c_{\mathbf{j}\sigma} + \text{H.c.} \right) \,, \quad H_\mu = -\mu \sum_{\mathbf{i}} n_{\mathbf{i}},$$

$$H_U = U \sum_{\mathbf{i}} n_{\mathbf{i}\uparrow} n_{\mathbf{i}\downarrow} \,, \quad H_V = \frac{V}{d} \sum_{\langle \mathbf{ij} \rangle} n_{\mathbf{i}} n_{\mathbf{j}} \,.$$

Here $c^\dagger_{\mathbf{i}\sigma}$ ($c_{\mathbf{i}\sigma}$) creates (destroys) an electron with spin σ at site $\mathbf{i}$, $n_{\mathbf{i}\sigma} \equiv c^\dagger_{\mathbf{i}\sigma} c_{\mathbf{i}\sigma}$, $n_{\mathbf{i}} \equiv n_{\mathbf{i}\downarrow} + n_{\mathbf{i}\uparrow}$ and d is the space dimension. In the sum over bonds $\langle \mathbf{ij} \rangle$ in H_t and H_V, it is understood that $\mathbf{i}$ and $\mathbf{j}$ are nearest neighbors and that every bond is counted only once. The grand canonical Hamiltonian (1) describes hopping of electrons (H_t), interacting with each other through on-site (H_U) and nearest-neighbor (H_V) Coulomb repulsion. For simplicity we assume that the lattice has a (hyper-)cubical structure. The prefactors in H_t and H_V are chosen such that a finite, nonvanishing energy contribution is obtained for $d \to \infty$.[15,16] Below we set $t = 1$ to fix the energy scale. Moreover, we consider only $U > 0$ and $V > 0$, since we assume Coulomb *repulsion*, but the results are valid in a wider range of parameters (see the discussion). The

 ©1994 The American Physical Society

original Hubbard model corresponds to $V = 0$ in (1). In this paper, we investigate the extended Hubbard model at weak coupling ($U, V \downarrow 0$), keeping the ratio

$$v = V/U$$

fixed. In order to obtain symmetry breaking at low temperatures, even for $U, V \downarrow 0$, we focus on the half-filled band ($n = 1$), which corresponds to a chemical potential $\mu = \frac{1}{2}U + 2V$.

The extended Hubbard model has been intensively studied previously, both analytically (at weak[17] and at strong[18,19] coupling) and numerically (usually at half[20,21] or at quarter[22] filling). These studies have been carried out primarily in low dimensions, but some analytical results for the ground state in higher dimensions ($d \geq 3$) are also available.[18,19] As a result of this work, it is well known that the ground state of the extended Hubbard model exhibits a transition between a spin and a charge-density-wave phase at $v \simeq \frac{1}{2}$ in all dimensions. These phases will be referred to as SDW and CDW throughout. On the basis of the Mermin-Wagner theorem,[5] which excludes long-range order at positive temperatures in $d \leq 2$, a mean field description of the extended Hubbard model (such as the Hartree-Fock approximation) is meaningful only in higher dimensions ($d \gtrsim 3$). The Hartree-Fock approximation for the extended Hubbard model was considered, e.g., in Ref. 23.

In this paper, we study the extended Hubbard model beyond the mean field approximation. Our aim is to obtain *exact* results in the weak-coupling limit ($U, V \downarrow 0$). Below we show that, to obtain exact results, one has to go to *second order* in perturbation theory. The Hartree (or Hartree-Fock) approximation by itself does *not* yield exact results for $U, V \downarrow 0$. This is even true in the limit of high dimensions, where various other mean field results for classical[24] and quantum mechanical[25] systems are known to be exact. Our main result is that the exact results for the critical temperature and the order parameter differ from the Hartree predictions by a factor $q(v)$ of order *unity*. The renormalization factor $q(v)$ cannot, in general, be calculated exactly in finite dimensions (such as $d = 3$). However, we show below that $q(v)$ can be calculated exactly in $d = \infty$; approximate results for finite-dimensional systems can then be obtained in a systematic $1/d$ expansion.

The starting point of our investigations (but not their goal) is therefore the infinite dimensional limit. This limit was introduced several years ago by Metzner and Vollhardt[15,26] as an approach to correlated Fermi systems on a lattice. The infinite-dimensional approach has yielded various valuable results, such as the exact solution of the Falicov-Kimball model by Brandt and Mielsch,[27] its relation to exact mean field theories,[28,29] and the mapping of Hubbard-type models to single impurity problems.[27,30,31] Unfortunately one of the most interesting goals, the exact (analytical) solution of the Hubbard model in $d = \infty$, still seems far out of reach. Recently, this shortcoming was partly made up for by the beautiful numerical results on the infinite-dimensional Hubbard model.[32–35] However, analytical results remain of interest, since the numerical simulations cannot cover too small or too large values of the interaction, or, for instance, the $T \to 0$ limit. Part of the intention of this paper is to add to the available analytical information about Hubbard-type models in higher dimensions.

The thermodynamics of the extended Hubbard model at small U and V can be determined by applying perturbation theory. The small parameters are, first, the interaction strengths U and V and, second, the inverse dimension $1/d$. The starting point of the perturbation expansion is the Hartree-Fock, or rather the Hartree approximation: We shall find below that the Fock contribution to T_c and to the order parameter is small compared to the Hartree contribution, of relative order U/d. However, the *standard* perturbation expansion around the Hartree solution, which is self-consistent only to linear order in the interaction, would lead to incorrect results. Instead one finds (by using self-consistent second-order perturbation theory) that the results, from the Hartree approximation are renormalized by a factor of the order of *unity*, even for $d \to \infty$ and in the limit $U, V \downarrow 0$.

To obtain these results, we proceed as follows. First, in Sec. II, we summarize the most important results from the Hartree approximation, notably those for the critical temperature, the order parameter, and the free energy gain due to symmetry breaking, analyzed in the limit $U, V \to 0$. Then, in Sec. III, we discuss the perturbation expansion at small U and V, including all diagrams which contribute to *second* order in U and V and up to *first* order in $1/d$. The calculation of these diagrams is discussed in Sec. IV. Finally, in Sec. V, we combine the results for the various diagrams and give explicit expressions for thermodynamical quantities, valid in the limit $U, V \to 0$ and including the $1/d$ corrections. We end with a discussion and a summary. Technical details are deferred to the appendixes.

II. THE HARTREE APPROXIMATION

The Hartree approximation is obtained by decoupling the interaction terms in H_U and H_V in (1):

$$n_{\mathbf{i}\sigma} n_{\mathbf{j}\sigma'} \to \langle n_{\mathbf{i}\sigma} \rangle n_{\mathbf{j}\sigma'} + n_{\mathbf{i}\sigma} \langle n_{\mathbf{j}\sigma'} \rangle - \langle n_{\mathbf{i}\sigma} \rangle \langle n_{\mathbf{j}\sigma'} \rangle \,. \tag{2}$$

Since we consider half filling, we make the usual assumption[36] that the average density has the form

$$\langle n_{\mathbf{i}\sigma} \rangle = \tfrac{1}{2}(1 + \lambda r_\sigma \Delta) \,, \tag{3}$$

where $\lambda = +1$ on one sublattice [labeled by $(+)$], and $\lambda = -1$ on the other [labeled by $(-)$]. The symmetry between $\uparrow$ and $\downarrow$ electrons implies that either $r_\sigma = 1$ [which corresponds to a charge density wave (CDW)], or $r_\sigma = \sigma$ (which corresponds to antiferromagnetism).[37] The order parameter Δ is denoted by Δ^H in the Hartree approximation, and can be calculated from the consistency requirement $\langle n_{\mathbf{i}\uparrow} \rangle_H = \frac{1}{2}(1 \pm \Delta^H)$ if $\mathbf{i} \in (\pm)$. As usual there are two solutions: a trivial solution $\Delta^H = 0$ and a nontrivial solution $\Delta^H > 0$ that has a lower (Hartree) free energy for $T < T_c^H$, where T_c^H is the Hartree critical

temperature. We focus on the nontrivial solution below.

What does the Hartree approximation predict? Below we give the results for the critical temperature, the order parameter, and the free energy gain due to symmetry breaking, calculated for a d-dimensional hypercubical lattice in the limit $U, V \to 0$. Details concerning the asymptotic analysis for $U, V \to 0$ can be found in Appendix A, Sec. A 4.

We start with the critical temperature T_c^H, which can be determined by putting $\Delta^H(T_c) = 0$ in (A7) and solving for T_c as a function of U and V. One finds that the critical temperature is exponentially small for $U, V \to 0$:

$$k_B T_c^H \sim \exp\left(I_d - \frac{1}{2\alpha U \nu_d(0)}\right) \qquad (U, V \to 0)\,. \quad (4)$$

For small U, the corrections to the right hand side are exponentially small, of order $(k_B T_c)^2$. The parameter α in (4) is given by $\alpha = 2v - \frac{1}{2}$ in the CDW and by $\alpha = \frac{1}{2}$ in the antiferromagnetic (SDW) phase. In general dimensions $d \geq 3$ the constant I_d can be expressed in terms of an integral,

$$I_d = \int_0^\infty dy\, \frac{1}{y}\left(\tanh y - 1 + \frac{\nu_d(y)}{\nu_d(0)}\right) - \ln 2, \quad (5)$$

where $\nu_d(y)$ is the density of states. In high dimensions ($d \gg 1$) the constant I_d can be calculated explicitly. Including the $1/d$ corrections one finds

$$I_d = \tfrac{3}{2}\ln 2 + \tfrac{1}{2}\gamma - \ln\pi + \frac{1}{4d} + O(d^{-2})\,, \quad (6)$$

where $\gamma \simeq 0.577$ is Euler's constant. The numerical value of I_d in (6) is $I_d \simeq 0.1836 + 1/4d$.

The order parameter, too, is exponentially small as a function of U and V. The temperature dependence of $\Delta^H(T)$ can most conveniently be formulated by introducing a rescaled order parameter $\delta \equiv \frac{1}{2}\alpha U \Delta^H / k_B T_c^H$ and a rescaled temperature $\theta \equiv T/T_c^H$. These rescaled quantities are for $U \to 0$ related by

$$0 = \int_0^\infty dy \left[\frac{\tanh\left(\sqrt{y^2+\delta^2}\,/\theta\right)}{\sqrt{y^2+\delta^2}} - \frac{\tanh y}{y}\right]. \quad (7)$$

Note that the rescaled order parameter $\delta(\theta)$ in (7) has the same form for all values of the interaction ratio v. Starting from (7), $\delta(\theta)$ can be calculated numerically. The result is presented as Fig. 1. In fact, the relevance of Fig. 1 extends beyond the Hartree approximation: Below we shall see that the *exact* order parameter of the extended Hubbard model, after proper rescaling, also has the form of Eq. (7) or, equivalently, Fig. 1. The limiting behavior of $\delta(\theta)$ for $\theta \downarrow 0$ and $\theta \uparrow 1$ can be calculated analytically. For $\theta \downarrow 0$ one finds that $\delta(\theta)$ approaches the limiting value $\delta(0) = \frac{1}{2}\pi e^{-\gamma} \simeq 0.882$ exponentially, where $\gamma = 0.577\cdots$ is Euler's constant. This implies that the gap ratio $2\alpha U \Delta^H(0)/k_B T_c^H$ is exactly given by $2\pi e^{-\gamma} \simeq 3.5285$, independent of v. This result for the gap ratio is *identical* to the standard[38] BCS result for this quantity. For $\theta \uparrow 1$ one obtains mean field critical behavior, $\delta(\theta) \sim A(1-\theta)^{1/2}$ with $A \simeq 1.53$. Details can be found in Appendix A 4.

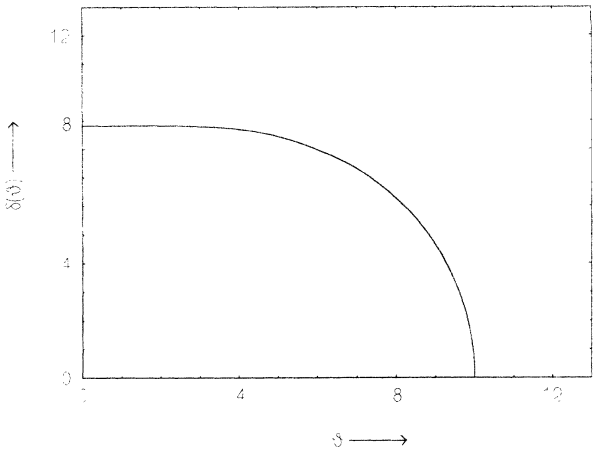

FIG. 1. The order parameter as a function of temperature, expressed in the rescaled variables $\delta \equiv \frac{1}{2}\alpha U \Delta / k_B T_c$ and $\theta \equiv T/T_c$.

The gain in free energy Ω_S^H due to symmetry breaking can also be calculated. For small U and V one finds (see Appendix A 4) that

$$\Omega_S^H(T) \sim -\alpha^2 U^2 (\Delta^H)^2 \nu_d(0) \Phi(\theta) \qquad (U \downarrow 0)\,, \quad (8)$$

where

$$\Phi(\theta) \equiv \int_0^\infty dy \left[\frac{2\theta}{\delta^2} \ln\left(\frac{\cosh(\sqrt{y^2+\delta^2}/\theta)}{\cosh(y/\theta)}\right) - \frac{\tanh y}{y}\right].$$

Note that the *lowest* free energy is obtained for the state with the *largest* value of α. This illustrates the well-known fact[23] that the system is in the CDW phase for $v > \frac{1}{2}$ and in the SDW phase for $v < \frac{1}{2}$, at least in the Hartree approximation.

III. PERTURBATION THEORY AT SMALL U AND V

The Hartree result (8) for the free energy gain due to symmetry breaking implies that one *cannot* use standard perturbation theory around the Hartree solution to study the fluctuations. The reason is that the contribution of the second-order diagrams to the free energy gain is also of order $U^2(\Delta^H)^2$ (see below). Hence the thermodynamics at small U and V has to be determined self-consistently from the Hartree contribution and the fluctuations together. There are various equivalent ways to do this. Below we will use a method proposed by Georges and Yedidia.[39] An alternative, which leads to the same result, is the self-consistent perturbation scheme of Bickers and Scalapino,[40] which is a conserving approximation in the spirit of Baym and Kadanoff.[41]

The method of Georges and Yedidia[39] is based on an expansion of the free energy per site $f(U, V, \Delta)$ in powers of U and V at a fixed value of the order parameter Δ:

$$f(U,V,\Delta) = \tilde{f}_0(\Delta) + U\tilde{f}_1(\Delta) + U^2\tilde{f}_2(\Delta) + \cdots \equiv f_0 + f_1 + f_2 + \cdots . \quad (9)$$

The functions $\tilde{f}_n(\Delta)$ in (9) depend implicitly on v and T. The order parameter in (9) is kept fixed by introducing a Lagrange parameter $h(U)$, which couples linearly to the staggered magnetization (in the SDW case) or to the staggered charge density (in the CDW case). For the purposes of this paper, we need a generalization of Ref. 39, tailored to the extended Hubbard model in position space and at positive temperatures. The necessary formalism can be found in Appendix B.

According to Appendix B, the contributions f_n to the free energy per site are for $n = 0, 1, 2$ given by

$$f_0 = h_0\Delta - \frac{4}{\beta}\int_0^\infty d\varepsilon\, \nu_d(\varepsilon) \ln\left[2\cosh\left(\tfrac{1}{2}\beta\eta_\varepsilon\right)\right] , \quad (10a)$$

$$f_1 = \tfrac{1}{4}U + V - \tfrac{1}{2}\alpha U\Delta^2 - 2V[G_1(0)]^2 , \quad (10b)$$

$$f_2 = -\frac{1}{2\beta}\int_0^\beta\int_0^\beta d\tau_1 d\tau_2 \,\langle[\tilde{H}_U(\tau_1) + \tilde{H}_V(\tau_1)] \times[\tilde{H}_U(\tau_2) + \tilde{H}_V(\tau_2)]\rangle_0^c . \quad (10c)$$

The various contributions f_n depend on the field $h_0 = h(0)$, which in turn depends upon Δ through the consistency relation (B3). The optimal (equilibrium) value of Δ is determined by minimization of the free energy at fixed (U,V,T):

$$0 = \frac{df}{d\Delta} = \frac{\partial f}{\partial h_0}\frac{dh_0}{d\Delta} + \frac{\partial f}{\partial \Delta} . \quad (11)$$

The quantity $G_1(0)$ in f_1 is the Hartree Green function $G_{\mathbf{ij}}(\tau)$ for nearest neighbors $\mathbf{i}$ and $\mathbf{j}$ and $\tau = 0$. The factors $\tilde{H}_U$ and $\tilde{H}_V$ in f_2 represent the fluctuations in H_U and H_V, see the definition (B4). The average $\langle\cdots\rangle_0^c$ refers to connected diagrams, which are to be calculated using Hartree Green functions with gap parameter h_0.

The various diagrams that have to be calculated in this approach (up to second order in U and V and up to first order in $1/d$) are listed in Fig. 2. A vertex H_U is represented by a dashed line, a vertex H_V by a wiggly line. There is one first-order diagram [diagram (a), the Fock term]. Diagrams (b)–(e) correspond to the various second-order diagrams. We also listed an example of a higher-order diagram, (f), which can be shown to be small. The calculation of these diagrams is discussed below, in Sec. IV.

The basic simplification occurring in high dimensions is that the Green functions $\langle T_\tau c_{\mathbf{j}+\mathbf{s},\sigma}(\tau)c^\dagger_{\mathbf{j}\sigma}(0)\rangle$ in position space fall off very rapidly with distance ($\propto d^{-|\mathbf{s}|/2}$ as $d \to \infty$). As a consequence of this rapid falloff of the Green functions, it becomes possible to explicitly evaluate diagrams in high dimensions, whose calculation in $d = 3$ would have been either impossible or at least numerically very costly. The physical idea is now that summation of the first few terms in the $1/d$ expansion of a diagram in high dimensions yields a good approximation to the value of that diagram in $d = 3$. As an example, consider the general second-order diagram of order U^2, containing two Hubbard-interactions with site labels

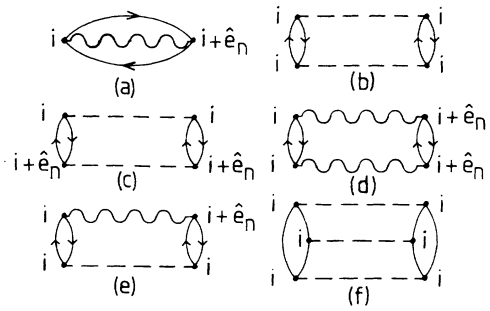

FIG. 2. Various diagrams encountered in perturbation theory at constant order parameter. The dashed line represents the Hubbard interaction $\tilde{H}_U$, while $\tilde{H}_V$ is represented by a wiggly line. The vertices are labeled by site indices; here, $\hat{e}_n$ is one of the $2d$ possible lattice vectors.

$\mathbf{i}$ and $\mathbf{j}$, respectively [the diagrams (a) and (b) in Fig. 2 are special cases, corresponding to $|i-j| = 0, 1$]. Since the U^2 diagram contains four lines, its value is proportional to $(d^{-|\mathbf{s}|/2})^4 = d^{-2|\mathbf{s}|}$, where $\mathbf{s} \equiv \mathbf{i} - \mathbf{j}$. For each $\mathbf{i}$ the number of different ways to choose a $\mathbf{j}$ at distance $|\mathbf{s}|$ is proportional to $d^{|\mathbf{s}|}$. Thus, the total contribution from all sites at a distance $|\mathbf{s}|$ is $\propto d^{-|\mathbf{s}|}$. Hence only the terms corresponding to $|\mathbf{s}| = 0, 1$ are needed to calculate the U^2 diagram up to $O(1/d)$. Along similar lines one concludes that the only first- and second-order diagrams contributing to the free energy up to $O(1/d)$ are those given in Fig. 2(a)–(e). All these diagrams can be calculated if one knows the Green functions for $|\mathbf{s}| = 0, 1$. The explicit form of these Green functions is given in Appendix A 2.

IV. CALCULATION OF DIAGRAMS

Of all diagrams listed in Fig. 2, diagrams (a), (b), and (f) are special. Diagram (a), the Fock term, is the only first-order diagram to be calculated; its evaluation is (relatively) simple and instructive. Diagram (b) is numerically the most important diagram in high dimensions: it yields a contribution of order *unity* as $d \to \infty$, while the other diagrams are smaller by a factor of either $1/d$ or U. Diagram (f) is of interest, since it leads to a stabilization of the SDW phase and hence to an upward shift of the SDW-CDW-phase boundary in the phase diagram. The calculation of diagrams (a), (b), (f) will therefore be discussed in some detail (technical details can be found in Appendix C). Results for the other diagrams will simply be stated.

Let the contribution to the free energy f of diagram ν ($\nu = a, \cdots, f$) be given by f_ν. It turns out to be convenient to calculate not f_ν itself, but instead its derivative

$$B_\nu(h_0,\beta) = \frac{1}{h_0}\frac{\partial f_\nu}{\partial h_0} . \quad (12)$$

One reason is, that one needs the derivative to determine the equilibrium value of Δ, see (11). Another reason is that it turns out to be easy to determine the free energy

gain $f_\nu(h_0,\beta) - f_\nu(0,\beta)$ from B_ν by integration in the end.

In the calculations of diagrams, it is convenient[42] to restrict consideration to those solutions $h_0(U,T)$ of Eq. (11) which have the same exponential U dependence as the solution of first-order perturbation theory. In particular, we assume for the ground state,

$$\ln h_0(T=0) \sim -\frac{1}{2\alpha U \nu_d(0)} \qquad (U \to 0) \,. \tag{13}$$

No assumptions are made concerning the prefactor of the exponential U dependence. Concerning the critical temperature we assume that $k_B T_c$ is of the same order of magnitude as the gap h_0 in the ground state, so that $\beta_c h_0(T=0) = O(1)$. Physically this is obvious. These assumptions will be justified *a posteriori*, since the solution for $h_0(T)$, to be found below, has the stated properties.

From the last term in f_1 in (10b) it is clear that the Fock contribution to the free energy is given by $f_a = -2V[G_1(0)]^2$, where $G_1(0)$ follows from Appendix A 2 as

$$\begin{aligned} G_1(0) &= -\frac{1}{\sqrt{2d}} \int_0^\infty d\varepsilon \; \nu_d(\varepsilon) \frac{\varepsilon^2}{\eta_\varepsilon} \tanh\left(\tfrac{1}{2}\beta\eta_\varepsilon\right) \\ &\equiv -\frac{1}{\sqrt{2d}} J(h_0^2,\beta) \,. \end{aligned}$$

Hence f_a can also be written as

$$f_a = -\frac{V}{d}\left[J(h_0^2,\beta)\right]^2 \,, \tag{14}$$

and, consequently,

$$B_a(h_0,\beta) = -\frac{4V}{d} J(h_0^2,\beta) J'(h_0^2,\beta) \,, \tag{15}$$

where we defined $J' \equiv \partial J/\partial h_0^2$. The calculation of B_a in (15) is discussed in Appendix C. It is shown there that, to dominant order in U, one obtains a very simple result:

$$B_a(h_0,\beta) \sim \frac{v}{\sqrt{2\pi}\alpha d} \qquad (T < T_c) \,. \tag{16}$$

This result is characteristic for many calculations in the limit $U \to 0$: the right hand side of Eq. (16) is *independent* of temperature. In fact, the dominant temperature dependence in B_a appears only in the dominant correction terms to (16), which are of relative order U.

We turn to the calculation of diagram (b), which describes the fluctuations in H_U at a given site. Diagram (b) is numerically important, since it is the only second-order diagram in Fig. 2 that survives in $d = \infty$. Since we are interested in the thermodynamics up to $O(d^{-1})$, we have to calculate diagram (b) *including its* $1/d$ *corrections.*

The integral form of diagram (b) is

$$\begin{aligned} f_b = -\frac{U^2}{4\beta} \int_0^\beta d\tau_1 \int_0^\beta d\tau_2 \sum_\lambda G^\lambda_{0\uparrow}(\tau_1-\tau_2) \\ \times G^\lambda_{0\uparrow}(\tau_2-\tau_1) G^\lambda_{0\downarrow}(\tau_2-\tau_1) G^\lambda_{0\downarrow}(\tau_1-\tau_2) \,. \end{aligned} \tag{17}$$

Since the Green functions for even values of ℓ have the symmetry properties $G^\lambda_{\ell\sigma}(\tau) = r_\sigma G^\lambda_{\ell\uparrow}(r_\sigma\tau)$ and $G^{-\lambda}_{\ell\sigma}(\tau) = -G^\lambda_{\ell\sigma}(-\tau)$ (see Appendix A 2), Eq. (17) reduces to

$$\begin{aligned} f_b &= -\frac{U^2}{2\beta} \int_0^\beta d\tau_1 \int_0^\beta d\tau_2 \left[G^+_{0\uparrow}(\tau_1-\tau_2) G^+_{0\uparrow}(\tau_2-\tau_1)\right]^2 \\ &= -\frac{U^2}{2} \int_0^\beta d\tau \; \left[G_0(\tau) G_0(-\tau)\right]^2 \\ &\equiv -\frac{U^2}{2} \mathcal{I}_b(\beta) \,. \end{aligned} \tag{18}$$

In the second step we used the periodicity of the integrand as a function of $\tau_1 - \tau_2$ and we simplified the notation to $G^+_{0\uparrow}(\tau) \equiv G_0(\tau)$. Details concerning the evaluation of the integral $\mathcal{I}_b(\beta)$ can be found in Appendix C. The main result for f_b, or rather for its derivative $B_b(h_0,\beta)$ is

$$B_b(h_0,\beta) \sim \gamma_d/\alpha^2 \qquad (U \to 0) \,, \tag{19}$$

where the constant γ_d is given in (C7). Again the most striking feature in (19) is that $B_b(h_0,\beta)$ is *independent* of temperature for all $T < T_c$. In fact the temperature dependence of $B_b(h_0,\beta)$ enters only to linear order in U, due to the first line on the right in (C8). The situation here is thus completely analogous to that for diagram (a), where the temperature dependence of $B_a(h_0,\beta)$ was also suppressed by one power of U.

Next we summarize the results for diagrams (c)–(e).

Diagram (c) describes fluctuations due to Hubbard interactions at neighboring sites. The diagram is of order $O(d^{-1})$, since it contains four nearest-neighbor Green functions [yielding a factor $(1/\sqrt{d})^4 = d^{-2}$] and all possible nearest-neighbors are summed over (yielding a factor d). The expression for diagram (c) in terms of Green functions is

$$\begin{aligned} f_c &= -U^2 d \int_0^\beta d\tau \; \left[G_1(\tau) G_1(-\tau)\right]^2 \\ &= -U^2 d \int_0^\beta d\tau \; \left[G_1(\tau)\right]^4 \,, \end{aligned} \tag{20}$$

which is of $O(U^2/d)$, since $G_1(\tau) = O(d^{-1/2})$. The form of (20) is very similar to that of Eq. (18) for diagram (b), the main difference being that G_0 is replaced by G_1. However, this difference leads to a qualitatively different result for the derivative $B(h_0,\beta)$: whereas B_b is of $O(1)$ for $U \to 0$, one finds that

$$B_c(h_0,\beta) = O(U/d) \qquad (T \le T_c) \,, \tag{21}$$

which is smaller than $B_b(h_0,\beta)$ by a factor of U for $U \to 0$. Hence diagram (c) is *negligibly small* in the limit $U \to 0$. The difference between diagram (a) and (c) comes about because for $\ell = 1$ the term proportional to Q_ℓ in (A5) vanishes. The term containing Q_ℓ distinguishes the two sublattices ($\lambda = \pm$) and yields the dominant contribution to diagrams involving $G_0(\tau)$.

Diagram (d) describes the $1/d$ corrections due to fluc-

tuations in H_V. The only contribution to order $1/d$ comes from the term with equal site indices at both vertices; all other terms are smaller by at least one power of $1/d$. The $1/d$ correction due to diagram (d) is therefore given by

$$f_d = -\frac{2V^2}{d}\int_0^\beta d\tau\ [G_0(\tau)G_0(-\tau)]^2 = -\frac{2V^2}{d}\mathcal{I}_b(\beta)\ ,$$

so that f_d is simply equal to $4v^2 f_b/d$. The immediate consequence for $B_d(h_0,\beta)$ is

$$B_d(h_0,\beta) = \frac{4v^2\gamma_\infty}{\alpha^2 d} \qquad (T \le T_c)\ , \tag{22}$$

which is again temperature independent for $T \le T_c$.

Diagram (e) describes the fluctuations due to mixing of H_U and H_V. The main contribution comes from terms where the lattice site, connected to H_U, is equal to one of the sites connected to H_V. The expression for diagram (e) in terms of Green functions is given by

$$f_e = -4UV\int_0^\beta d\tau\ G_0(\tau)G_0(-\tau)G_1(\tau)G_1(-\tau)\ ,$$

and the resulting expression for $B_e(h_0,\beta)$ is

$$B_e(h_0,\beta) = \frac{v}{\alpha^2 d}\left(\gamma_\infty - \frac{1}{\sqrt{2\pi}}\right) \qquad (T \le T_c)\ , \tag{23}$$

which is temperature independent and of $O(d^{-1})$ for $U \to 0$.

Finally, as an example of a higher-order diagram, we consider the third-order diagram (f) in Fig. 2 and show that the corresponding derivative $B_f(h_0,\beta)$ is negligibly small compared to the second-order contributions. In fact (for reasons to be explained in the discussion) diagram (f) has interesting implications for the phase diagram of the extended Hubbard model at finite U and V, so that its calculation is very much worthwhile. The integral form of diagram (f) can be expressed in terms of the Green function $G_0(\tau) = G^+_{0\uparrow}(\tau)$ as

$$f_f = \frac{U^3 r_\downarrow}{6\beta}\int_0^\beta d\tau_3\int_0^\beta d\tau_2\int_0^\beta d\tau_1\ [T(\tau_1,\tau_2,\tau_3)]^2\ , \tag{24}$$

where

$$T(\tau_1,\tau_2,\tau_3) \equiv G_0(\tau_{21})G_0(\tau_{32})G_0(\tau_{13}) + G_0(\tau_{12})G_0(\tau_{23})G_0(\tau_{31})$$

and $\tau_{21} = \tau_2 - \tau_1$, etc. The factor $r_\downarrow$ in the right hand side of (24) is important because it distinguishes the CDW ($r_\downarrow = 1$) and SDW ($r_\downarrow = -1$) phases. It comes about because diagram (f) has three $\uparrow$ and three $\downarrow$ lines, yielding a factor $r_\uparrow^3 r_\downarrow^3 = r_\downarrow$ to (24). In Appendix C we show that the free energy contribution due to diagram (f) can be calculated explicitly. The result has a very simple form, namely, $f_f = \frac{1}{2}U r_\downarrow \bar{C}_f h_0^2$, where the (positive) constant $\bar{C}_f$ is explicitly known in the form of an integral (see Appendix C). As a consequence, the derivative $\bar{B}(h_0,\beta)$, corresponding to diagram (f), is given by $B_f = r_\downarrow \bar{C}_f U$ for $U \downarrow 0$. This is smaller by one power of U than the contributions B_ν of the diagrams (a),(b),(d),(e), so that in the limit $U \downarrow 0$ diagram (f) can be neglected. However, at small but finite U diagram (f) nevertheless has important implications. We will come back to this in the discussion.

V. COMBINATION OF RESULTS

Combination of the results for $B_\nu(h_0,\beta)$, obtained above for the various diagrams (a)–(e) yields the following results. If we define the free energy correction, due to these diagrams, by

$$\bar{f} \equiv f_a + f_b + f_c + f_d + f_e\ ,$$

then the derivative

$$\bar{B}(h_0,\beta) \equiv \frac{1}{h_0}\frac{\partial \bar{f}}{\partial h_0} \sim \bar{C} \qquad (U \to 0) \tag{25}$$

is temperature independent for $T \le T_c$, the constant $\bar{C}$ being given by

$$\bar{C} = \frac{v}{\sqrt{2\pi}\alpha d} + \frac{\gamma_d}{\alpha^2} + \frac{4v^2\gamma_\infty}{\alpha^2 d} + \frac{v}{\alpha^2 d}\left(\gamma_\infty - \frac{1}{\sqrt{2\pi}}\right)\ . \tag{26}$$

The order parameter Δ is determined by minimization of the total free energy, which is the sum of the Hartree contribution and the diagrammatic corrections: $f = f^H + \bar{f}$. The resulting equation for Δ is

$$0 = \frac{df}{d\Delta} = h_0 - \alpha U\Delta + \bar{C}h_0\frac{dh_0}{d\Delta}\ , \tag{27}$$

where h_0 is related to Δ by (B3). Equation (27) can be rewritten as

$$h_0 \sim \alpha U\Delta/\left(1 + \bar{C}dh_0/d\Delta\right)\ .$$

From (B3), in combination with (13), we know that $dh_0/d\Delta \sim \alpha U$, so that

$$h_0 = \alpha^* U\Delta\ , \tag{28a}$$

$$\alpha^* \sim \alpha - \alpha^2 U\bar{C} + \cdots\ , \tag{28b}$$

where the dots $(\cdots)$ are small compared to U if $U \to 0$. Insertion of (28a) into (B3), and comparison with Eq. (A7) for the order parameter in Hartree approximation, shows that Δ has the *same* form as Δ^H if in addition one replaces $\alpha \to \alpha^*$.

As the immediate result one finds that the actual critical temperature T_c and the order parameter Δ can be expressed in terms of their Hartree equivalents and a scaling factor

$$q(v) \equiv e^{-\bar{C}/2\nu_d(0)} = e^{-C_0 - C_1 d^{-1}}\ , \tag{29}$$

with

$$C_0 = \frac{1}{2\sqrt{2}\alpha^2} \ln \tan\left(\frac{3\pi}{8}\right) , \tag{30}$$

$$C_1 = \frac{(\alpha-1)v}{2\alpha^2} - \frac{1}{64\alpha^2} + C_0\left(\frac{3}{32} + v + 4v^2\right) .$$

Again C_0 can be cast into another form using $\tan(3\pi/8) = \sqrt{2}+1$. The constants C_0 and C_1 are strictly positive, so that $q(v) < 1$ for all $v \geq 0$. By replacing $\alpha \to \alpha^*$ in (4) one finds that the actual critical temperature T_c is reduced by a factor of q relative to the Hartree prediction T_c^H:

$$T_c \sim qT_c^H \qquad (U, V \downarrow 0) . \tag{31}$$

Similarly one finds that, if we redefine $\theta \equiv T/T_c$ and $\delta \equiv \frac{1}{2}\alpha U\Delta/k_BT_c$, the relation between δ and θ is precisely the same as in Eq. (7) for the Hartree approximation. As a consequence, the *exact* rescaled order parameter $\delta(\theta)$ has the same form as the rescaled Hartree order parameter, sketched in Fig. 1. Consequently the order parameter $\Delta(T)$ itself is reduced by a factor q relative to Δ^H, calculated at the higher temperature T/q, i.e.,

$$\Delta(T) \sim q\Delta^H(T/q) \qquad (U, V \downarrow 0) . \tag{32}$$

The free energy gain due to symmetry breaking follows immediately from (8) as

$$\begin{aligned} \Omega_S(T) &\sim -\alpha^2U^2[\Delta(T)]^2\nu_d(0)\Phi(\theta) \\ &\sim q^2\Omega_S^H(T/q) \qquad (U \to 0) . \end{aligned} \tag{33}$$

Since obviously $\Omega_S < 0$ for $T < T_c$ we conclude that symmetry breaking is stable also if fluctuations are taken into account. Moreover, the critical temperature T_c and the free energy gain $|\Omega_S|$ are largest if one chooses $\alpha = \max\{\frac{1}{2}, 2v - \frac{1}{2}\}$ in the expressions for C_0 and C_1 in (30). This shows that the first-order transition between the SDW and CDW phases, occurring at $v = \frac{1}{2}$ at the Hartree level, is robust against the inclusion of fluctuations and $1/d$ corrections, at least in the limit $U \downarrow 0$. A graphical representation of $C_0(v)$ and $C_1(v)$ can be found in Fig. 3. The resulting renormalization factor $q(v)$ in (29) is presented in Fig. 4 for $d = \infty$ and 3, respectively.

VI. DISCUSSION

I start the discussion by emphasizing the importance of these findings for finite dimensions and finite values of U and V. The effect of finite dimensionality has been taken into account in the framework of a $1/d$ expansion. The $1/d$ expansion shows that the renormalization factor $q(v)$ (which is strictly smaller than unity already in $d = \infty$) decreases even further if the dimensionality of the system is lowered. The implication is that the renormalization found here is *not* a peculiarity of high dimensions, but that in fact the Hartree predictions for, e.g., the three-dimensional system[43] are even more strongly renormalized for $U, V \downarrow 0$ than those in $d = \infty$. Similarly, our results have important implications for the relevance of Hartree calculations at finite values of the interaction: If the Hartree predictions are renormalized already for $U, V \downarrow 0$, where they are supposedly best, it is clear that they will also be renormalized at finite U and V. Hence, even if the Hartree approximation yields *qualitatively* correct results, *quantitatively* it is not a very good approximation, at least not for Hubbard-type models in their low-temperature phase. This point has perhaps not been sufficiently appreciated previously.

Consider again Fig. 3 for C_0 and C_1 and Fig. 4 for $q(v)$. The fact that C_0 and C_1 are positive for all v shows that fluctuations and finite dimensionality *reduce* the critical temperature and the order parameter, as one would expect. As one can see from Fig. 3, the $1/d$ corrections are largest for $v = \frac{1}{2}$, i.e., precisely at the SDW-CDW transition. The combined effect of fluctuations and finite dimensionality can be seen in Fig. 4. The renormalization effects, represented by $q(v)$, are generally much stronger in the SDW phase than in the CDW phase. In the SDW

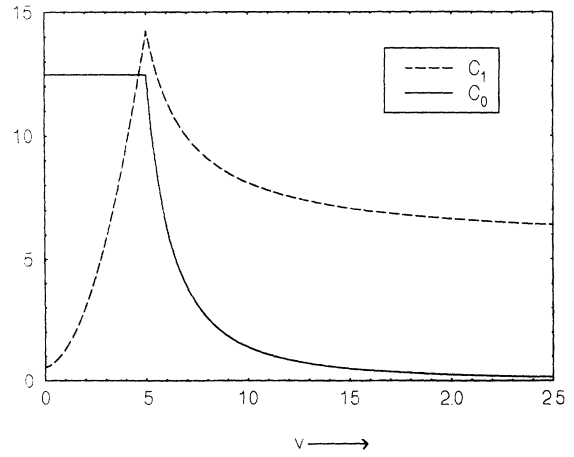

FIG. 3. The v dependence of the constants $C_0(v)$ and $C_1(v)$, showing clearly that C_0 and C_1 are positive and that the $1/d$ corrections are largest near the SDW-CDW transition.

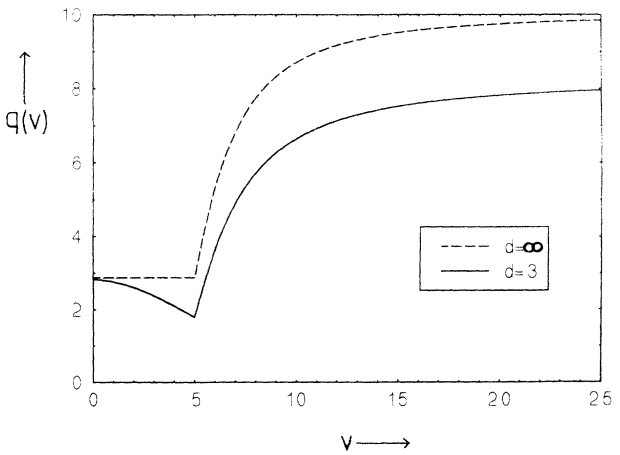

FIG. 4. The renormalization factor $q(v)$ in $d = 3$ and in $d = \infty$. Here $q(v)$ in $d = 3$ is determined from the $1/d$ expansion up to $O(1/d)$.

phase $q(v)$ is v independent for $d = \infty$; due to the $1/d$ corrections this is not true in any finite dimension, as is apparent from Fig. 4 for $d = 3$. In the SDW phase in $d = 3$ the renormalization factor drops below 0.2 for $v \simeq \frac{1}{2}$, so that near the SDW-CDW transition the Hartree results are off by a factor of more than five. Note that the $1/d$ corrections for the pure Hubbard model ($v = 0$) are very small: here $q(0) \simeq 0.288 - 0.016/d$. In the CDW phase the renormalization effects become weaker as v increases. They vanish for $v \to \infty$ only in $d = \infty$; in finite dimensions (e.g., in $d = 3$) renormalization effects are appreciable even at $v = \infty$.

Next I compare my results to existing numerical simulations. The most reliable simulation results are those obtained by various groups[32–35] for the Hubbard model in infinite dimensions.[44] In particular, Jarrell[32] calculated the critical temperature $T_c(U)$ for U values down to $U = 1/\sqrt{2}$ (in our units). As the result he finds that, at $U = 1/\sqrt{2}$, the Hartree critical temperature T_c^H is indeed renormalized by an effective q factor $q^{\text{eff}} \simeq 0.4$, in reasonable agreement with our result $q \simeq 0.288$ at $U = 0^+$. For the special case of the infinite dimensional Hubbard model it can be shown[45] that higher-order perturbative corrections to $q(0)$ lead to fair agreement with the Monte Carlo data for all $U \lesssim 2$ (again in our units). Unfortunately it is not possible to compare the order parameter curve of Fig. 1 to the Monte Carlo simulations, since none of the groups published data for the order parameter at small U.

The relevance of the results of Ref. 6 for superconductivity has recently been emphasized by Freericks.[45] At half filling the positive-U Hubbard model ($v = 0$) can be mapped to the negative-U Hubbard model[46] by a special particle-hole transformation.[47] As a consequence the superconducting transition temperature in the model with $U < 0$ differs from the BCS prediction by the *same* renormalization factor $q(v = 0)$ that was first presented in Ref. 6 for $U > 0$. Qualitatively, the same result (a renormalization of T_c and Δ by a factor of order unity) was obtained by Martín-Rodero and Flores,[48] who considered the negative-U Hubbard model in $d = 2$ using the local approximation.

In this paper, we assumed that the interaction parameters U and V are positive, corresponding to Coulomb repulsion. However, our results are in fact valid in a wider range of parameters. The relevance of this paper for the negative-U Hubbard model ($U < 0$, $V = 0$) has already been mentioned. From the phase diagram of the extended Hubbard model, sketched in Ref. 46, we further know that the CDW phase is stable in the region $U < 0$, $V > 0$. Inspection shows that all our results for the CDW phase are also valid in this region. Hence the renormalization factor $q(v)$ for $U < 0$, $V > 0$, is also given by (29), where now $v < 0$ and $\alpha = 2v - \frac{1}{2} < 0$. One easily verifies that the constants C_0 and C_1 are again strictly positive, so that T_c and Δ are reduced by the fluctuations and $1/d$ corrections. Similarly our results for the SDW phase (where $\alpha = \frac{1}{2}$) are valid whenever this phase is actually realized. The phase diagram of Ref. 46 shows that the SDW phase is stable in the region $U > 0$, $V < 0$, provided $|v|$ is not too large. Hence our results for $q(v)$ also apply to this range of parameter values. In this range, too, the constants C_0 and C_1 are strictly positive.

We now come back to the calculation of the third-order diagram (f) in Sec. IV. Diagram (f) is important for the ∞-dimensional model at small but finite values of U, since in $d = \infty$ it is the *only* surviving diagram to order U^3 and the leading diagram containing a factor $r_\downarrow$. This has several interesting consequences. To start with, we showed in Sec. IV that diagram (f) leads to a contribution $B_f(h_0, \beta) = r_\downarrow \bar{C}_f U$. This contribution is to be added to (25), implying that $\bar{C}$ in (26) is to be replaced by $\bar{C} + r_\downarrow \bar{C}_f U$. This combination is to be inserted into (29). Since $\bar{C}_f$ is strictly positive (see Appendix C), we conclude that the third order diagram implies a further *decrease* of T_c if $r_\downarrow$ is positive (i.e., in the CDW phase), but an *increase* of T_c if $r_\downarrow$ is negative (which happens in the SDW phase). This increase of T_c in third-order perturbation theory in the SDW phase was recently observed numerically by Freericks (Ref. 45). His result improves the agreement between perturbation theory and Jarrells Monte Carlo simulation.[32] Moreover, diagram (f) has another interesting implication: It gives rise to an upward shift of the phase boundary between the SDW and the CDW phases, which (up to second order in perturbation theory) is located exactly at $v = \frac{1}{2}$. This effect is due to the factor $r_\downarrow$ in (C9) or $B_f(h_0, \beta)$, which raises T_c (lowers the free energy) in the SDW phase but lowers T_c (raises the free energy) in the CDW phase. The upward shift of the phase boundary, which is demonstrated here at weak coupling in high dimensions, is well known in the one-dimensional system from the Monte Carlo simulations by Hirsch,[20] and has been demonstrated numerically in $d = 2$ by Zhang and Callaway.[49]

A technical remark concerning the perturbation scheme proposed in Ref. 39 is in order. The method of Ref. 39 leads to a systematic expansion in U *provided* one keeps the order parameter Δ fixed while taking the limit $U \downarrow 0$. However, in all practical applications[6,39,48] the equilibrium value of the order parameter is strongly U dependent for $U \downarrow 0$. As a result the systematic character of the perturbation expansion for the free energy is not guaranteed. In fact, we have shown in this paper that the expansion is indeed "mildly unsystematic," in the sense that several diagrams are smaller than they appear at first sight. For example, the first-order Fock diagram leads to a contribution to $q(v)$ of order unity, like most of the second-order diagrams, while the contribution to $q(v)$ of diagram (c), which is also a second-order diagram, is negligibly small for $U \downarrow 0$. A consequence of this mildly unsystematic character is that, in equilibrium, the expansion reduces to the *Hartree* rather than *Hartree-Fock* approximation to first order in U (see Appendix B).

The techniques which were applied in this paper to the extended Hubbard model can obviously also be used to study other, related models. One example is the model for spinless fermions.[50–52] This model can be viewed as a special case of the extended Hubbard model with only one spin species and hence without the local Hubbard interaction. It turns out that the calculations for spin-

less fermions are virtually identical to those carried out above for the extended Hubbard model. The connection between both models is explicitly demonstrated in Appendix D. The main result is that the Hartree predictions are renormalized for small interaction, as in (31), (32), and (33), but that the q factor for spinless fermions is close to unity: $q^{\mathrm{SF}} \sim \exp(-C_1' d^{-1})$ for $d \to \infty$ with the constant C_1' given in (D2). In fact the constant C_1' for spinless fermions is precisely twice the value C_1 one would obtain for the extended Hubbard model at $U = 0$. Hence $q^{\mathrm{SF}} = [q(v = \infty)]^2$. This expresses the physically obvious fact that the stronger the renormalization of the Hartree results due to fluctuations is, the lower the number of "colors" (spin species) in the model is.

VII. SUMMARY AND OUTLOOK

To summarize the results: We studied the thermodynamics of the extended Hubbard model at weak coupling on a hypercubic lattice in high dimension ($d \gg 1$). Special attention has been paid to the critical temperature T_c and to the order parameter $\Delta(T)$. These quantities have been calculated in second-order perturbation theory with respect to the interaction parameters U and V, and up to first order in $1/d$. Our most important result is that the Hartree results for T_c and $\Delta(T)$ are renormalized by a factor $q(v) < 1$ even at arbitrarily weak interaction ($U, V \downarrow 0$). For example, for the standard Hubbard model ($V = 0$) in $d = 3$ one finds $q \simeq 0.282$, so that the Hartree results are renormalized by a factor of more than three. This result is in agreement with existing Monte Carlo simulations. Up to second order in perturbation theory, the phase boundary between the SDW and the CDW phases remains fixed at $V/U = \frac{1}{2}$. We showed that an upward shift of the phase boundary is obtained if the *third* order in perturbation theory is also included. Furthermore, we found that the exact gap ratio $2\alpha U\Delta(0)/k_B T_c$ for $U \downarrow 0$ is *identical* to the gap ratio $2\pi e^{-\gamma} \simeq 3.5285$ found in Hartree approximation. The close relation between the renormalization effects in the extended Hubbard model and those for spinless fermions was pointed out.

The results of this work can be extended in various other directions. For instance, it would be interesting to investigate the renormalization effects in the superconducting phases of the extended Hubbard model with $V < 0$. Another extension would be to study the effect of other interactions on the phase diagram at small U and V. The calculations presented here can also be generalized to the non-half-filled band ($n \simeq 1$), or to the extended Hubbard model in the presence of a weak magnetic field. Work in these directions is underway.

ACKNOWLEDGMENTS

It is a pleasure to acknowledge helpful and stimulating discussions with D. Vollhardt, V. Janiš, and G. Uhrig (RWTH Aachen). I am grateful to A. Georges (Paris) for drawing my attention to Ref. 39. I am furthermore obliged to J. K. Freericks (University of California at Davis) for valuable correspondence on his work on superconductivity (Ref. 45) and on the comparison of calculated and observed Néel temperatures in the infinite dimensional Hubbard model. This work is supported in part by the Deutsche Forschungsgemeinschaft under SFB 341.

APPENDIX A: THE HARTREE APPROXIMATION, EXACT AND ASYMPTOTIC RESULTS

In this appendix we give the basic expressions for thermodynamic quantities and Green functions, needed in the text. We also derive asymptotic results for the critical temperature, order parameter and grand potential in the weak coupling limit.

1. Basic relations

The Hartree approximation to the extended Hubbard Hamiltonian (1) is defined by the decoupling scheme of Eq. (2). The expectation value of $n_{i\sigma}$ in (2) is given in (3) with $\Delta_\sigma = r_\sigma \Delta$ with $r_\sigma = \sigma$ for the spin-density wave (SDW) and $r_\sigma = 1$ for the charge-density wave (CDW). The chemical potential at half filling is in both cases given by $\mu = \frac{1}{2}U + 2V$.

Insertion of the decoupling (2) into (1) leads to a Hartree Hamiltonian of the form

$$H^{\mathrm{HF}} = H_t - \sum_{\sigma,\lambda} h_\sigma \lambda N_\sigma^\lambda + \tfrac{1}{2}\alpha U \mathcal{N}\Delta^2 - \mathcal{N}(V + \tfrac{1}{4}U) \,. \tag{A1}$$

Here N_σ^λ denotes the number of σ spins on the λ sublattice ($\lambda = \pm$) and $h_\sigma = r_\sigma h_0$ with $h_0 \equiv \alpha U \Delta$. The parameter α takes the value $\alpha = \frac{1}{2}$ in the SDW phase and $\alpha = 2v - \frac{1}{2}$ in the CDW phase. Fourier transformation of (A1) into $\mathbf{k}$ space yields

$$H^{\mathrm{HF}} = \tfrac{1}{2} \sum_{\mathbf{k}\sigma} H_{\mathbf{k}\sigma} + \tfrac{1}{2}\alpha U \mathcal{N}\Delta^2 - \mathcal{N}(V + \tfrac{1}{4}U) \,, \tag{A2}$$

where

$$H_{\mathbf{k}\sigma} = \varepsilon_{\mathbf{k}}(n_{\mathbf{k}\sigma} - n_{\mathbf{k}-\mathbf{Q}\sigma}) - h_\sigma(c_{\mathbf{k}\sigma}^\dagger c_{\mathbf{k}-\mathbf{Q}\sigma} + c_{\mathbf{k}-\mathbf{Q}\sigma}^\dagger c_{\mathbf{k}\sigma}) \,.$$

Here, $\varepsilon_{\mathbf{k}} = -2t \sum_{n=1}^d \cos(k_n)$ is the dispersion for $U = 0$. The Hamiltonian (A2) is diagonalized by a canonical transformation of the form $c_{\mathbf{k}\sigma} = a_{\mathbf{k}\sigma} d_{\mathbf{k}\sigma} + b_{\mathbf{k}\sigma} d_{\mathbf{k}-\mathbf{Q}\sigma}$. The real numbers $a_{\mathbf{k}\sigma}$ and $b_{\mathbf{k}\sigma}$ are given by

$$a_{\mathbf{k}\sigma} = \mathrm{sgn}(h_\sigma)\sqrt{\frac{\eta_{\mathbf{k}\sigma} + \varepsilon_{\mathbf{k}}}{2\eta_{\mathbf{k}\sigma}}} \;;\; b_{\mathbf{k}\sigma} = \mathrm{sgn}(\varepsilon_{\mathbf{k}})\sqrt{\frac{\eta_{\mathbf{k}\sigma} - \varepsilon_{\mathbf{k}}}{2\eta_{\mathbf{k}\sigma}}} \,,$$

where $\eta_{\mathbf{k}\sigma} \equiv \mathrm{sgn}(\varepsilon_{\mathbf{k}})\sqrt{\varepsilon_{\mathbf{k}}^2 + h_0^2}$. As a result, (A2) reduces to the form

$$H^{\mathrm{HF}} = \sum_{\mathbf{k}\sigma} \eta_{\mathbf{k}\sigma}\nu_{\mathbf{k}\sigma} + \tfrac{1}{2}\alpha U\mathcal{N}\Delta^2 - \mathcal{N}(V + \tfrac{1}{4}U) , \quad \text{(A3)}$$

where $\nu_{\mathbf{k}\sigma}$ is the number operator for the $d_{\mathbf{k}\sigma}$ particles, $\nu_{\mathbf{k}\sigma} = d^\dagger_{\mathbf{k}\sigma}d_{\mathbf{k}\sigma}$.

2. The Green functions

Since the Hamiltonian (A3) for the $d_{\mathbf{k}\sigma}$ particles is diagonal, one can immediately write down the corresponding Green functions:[1]

$$\langle T_\tau d_{\mathbf{k}\sigma}(\tau) d^\dagger_{\mathbf{k}'\sigma'}(\tau')\rangle = \delta_{\mathbf{k}\mathbf{k}'}\delta_{\sigma\sigma'} g_{\mathbf{k}\sigma}(\tau - \tau') , \quad \text{(A4)}$$

where

$$g_{\mathbf{k}\sigma}(\tau) = e^{-\eta_{\mathbf{k}\sigma}\tau}[\vartheta(\tau - 0^+)(1 - \langle\nu_{\mathbf{k}\sigma}\rangle) - \vartheta(0^+ - \tau)\langle\nu_{\mathbf{k}\sigma}\rangle] .$$

The Green functions of the $c_{\mathbf{i}\sigma}$ particles (in position space) can obviously be expressed as linear combinations of the Green functions in (A4). With the definition

$$G^\lambda_{\mathbf{l}\sigma}(\tau) \equiv \langle T_\tau c_{\mathbf{j}+\mathbf{l},\sigma}(\tau) c^\dagger_{\mathbf{j}\sigma}(0)\rangle \qquad (\mathbf{j} \in \lambda\text{-sublattice})$$

one finds that

$$G^\lambda_{\mathbf{l}\sigma}(\tau) = \frac{1}{\mathcal{N}}\sum_{\mathbf{k}} e^{i\mathbf{k}\mathbf{l}}\,(a_{\mathbf{k}\sigma} - \lambda b_{\mathbf{k}\sigma}) \times \left[a_{\mathbf{k}\sigma} - \lambda(-1)^{\mathbf{l}} b_{\mathbf{k}\sigma}\right] g_{\mathbf{k}\sigma}(\tau) .$$

In general dimensions this expression for $G^\lambda_{\mathbf{l}\sigma}$ still has the form of a complicated d-dimensional $\mathbf{k}$ integral. However, in the limit $d \to \infty$ this integral can be reduced to a (relatively) simple one-dimensional energy integral. We give only the result: With the definition $\ell \equiv |\mathbf{l}| \equiv \sum_{n=1}^d |l_n|$ for the length of $\mathbf{l}$ on the lattice one finds that $G^\lambda_{\mathbf{l}\sigma}(\tau)$ has the form

$$G^\lambda_{\ell\sigma}(\tau) = P_\ell(\tau;\beta) - \lambda h_\sigma Q_\ell(\tau;\beta) , \quad \text{(A5)}$$

where

$$P_\ell(\tau;\beta) = (2d)^{-\ell/2}\int_0^\infty d\varepsilon\, \nu_d(\varepsilon)\mathrm{He}_\ell(\varepsilon)\left[\mathrm{g}_\varepsilon(\tau) + \mathrm{g}_{-\varepsilon}(\tau)\right] ,$$

$$Q_\ell(\tau;\beta) = (2d)^{-\ell/2}\int_0^\infty d\varepsilon\, \nu_d(\varepsilon)\mathrm{He}_\ell(\varepsilon) \times \left[\mathrm{g}_\varepsilon(\tau) - \mathrm{g}_{-\varepsilon}(\tau)\right]/\eta_\varepsilon ,$$

if ℓ is even and

$$P_\ell(\tau;\beta) = -(2d)^{-\ell/2}\int_0^\infty d\varepsilon\, \nu_d(\varepsilon)\mathrm{He}_\ell(\varepsilon)\frac{\varepsilon}{\eta_\varepsilon} \times \left[g_\varepsilon(\tau) - g_{-\varepsilon}(\tau)\right]$$

$$Q_\ell(\tau;\beta) = 0$$

if ℓ is odd. Here $\mathrm{He}_\ell(\varepsilon)$ is a Hermite polynomial and $\nu_d(\varepsilon)$ is the density of states for $U = 0$, which is a Gaussian for $d \to \infty$, see (A9). The Green functions for $\ell = 0$ and $\ell = 1$ are special in the sense that (A5), with the expressions for P_ℓ and Q_ℓ given above, holds in all dimensions d, not just in $d = \infty$.

3. Thermodynamics

The thermodynamical results follow immediately from the Hamiltonian in the form (A3). The average number of $d_{\mathbf{k}\sigma}$ particles is $\langle\nu_{\mathbf{k}\sigma}\rangle = \left(e^{\beta\eta_{\mathbf{k}}} + 1\right)^{-1}$ and hence the grand potential per site is

$$\omega = \tfrac{1}{2}\alpha U\Delta^2 - (V + \tfrac{1}{4}U) - \frac{1}{\mathcal{N}\beta}\sum_{\mathbf{k}\sigma}\ln\left(1 + e^{-\beta\eta_{\mathbf{k}}}\right)$$
$$= \tfrac{1}{2}\alpha U\Delta^2 - (V + \tfrac{1}{4}U) - \frac{4}{\beta}\int_0^\infty d\varepsilon\, \nu_d(\varepsilon)\ln\left[2\cosh\left(\tfrac{1}{2}\beta\eta_\varepsilon\right)\right] . \quad \text{(A6)}$$

The consistency relation for the order parameter Δ follows from the condition $G^+_{0\uparrow}(\tau = 0) = -\frac{1}{2}(1 + \Delta)$. One finds that either $\Delta = 0$ (which is the solution in the high-temperature phase) or

$$1 = 2\alpha U\int_0^\infty d\varepsilon\, \nu_d(\varepsilon)\frac{\tanh(\frac{1}{2}\beta\eta_\varepsilon)}{\eta_\varepsilon} . \quad \text{(A7)}$$

The critical temperature $T_c = 1/k_B\beta_c$ is determined by $\Delta(T_c) = 0$ in (A7), i.e.,

$$1 = 2\alpha U\int_0^\infty d\varepsilon\, \nu_d(\varepsilon)\frac{\tanh(\frac{1}{2}\beta_c\varepsilon)}{\varepsilon} \equiv 2\alpha U J(\tfrac{1}{2}\beta_c) . \quad \text{(A8)}$$

These equations for ω, Δ, and T_c will be analyzed below for $U \downarrow 0$.

4. Asymptotic results for small U

We discuss the asymptotic behavior of the critical temperature T_c, the order parameter Δ, and the free energy gain due to symmetry breaking, in that order.

To obtain results for T_c we consider the function $J(\gamma)$ in (A8) for large γ; one finds that

$$J(\gamma) = \nu_d(0)\left(\ln\gamma + I_d + \ln 2\right) + O\left(\gamma^{-1}\right) ,$$

where the constant I_d is defined in (5). As a consequence, Eq. (A8) reduces to

$$1 = 2\alpha U\nu_d(0)\left(\ln\beta_c + I_d\right) + O\left(\beta_c^{-1}\right) ,$$

which is equivalent to Eq. (4) for T_c given in the text.

In general dimensions d the expression (5) for I_d is too complicated to be evaluated explicitly. The integral in (5) becomes tractable, however, in the limit $d \to \infty$, where the density of states, including the $1/d$ corrections, has the form

$$\nu_d(\varepsilon) = \nu_\infty(\varepsilon)\left[1 - \tfrac{1}{16d}(3 - 6\varepsilon^2 + \varepsilon^4)\right] . \quad \text{(A9)}$$

Here ν_∞ is the density of states in infinite dimensions, which is given by[15] $\nu_\infty(\varepsilon) = \frac{1}{\sqrt{2\pi}}e^{-\varepsilon^2/2}$. To calculate I_d in (5) we cut off the integral with an exponential factor

$e^{-\kappa y}$. The first term, containing $y^{-1}\tanh y$, can then be expressed in terms of gamma functions using formula (3.551.9) of Ref. 53. To calculate the second and the third term we use an algebraic cutoff y^{α}, with $\alpha \downarrow 0$. The second and the third term can then also be expressed in terms of gamma functions, whose asymptotic behavior is known for $\alpha \downarrow 0$. Combining results one obtains the result (6) in the limit $\kappa \downarrow 0$.

Next, we consider the order parameter $\Delta(T)$. A quick estimate of Δ for small U can be obtained by considering the ground state. For $T = 0$, or $\beta = \infty$, it follows from (A7) that

$$1 \sim 2\alpha U \int_0^{\infty} d\varepsilon\ \nu_d(\varepsilon)/\eta_{\varepsilon} \sim 2\alpha U \nu_d(0) \ln\left(\frac{1}{\alpha U \Delta}\right) \qquad (U \downarrow 0)\ .$$

Hence the gap $2\alpha U\Delta(0)$ is exponentially small if U is small, of the same order as $k_B T_c$.

To calculate the precise behavior of Δ, including its temperature dependence, we reconsider (A7) and subtract from it the T_c equation (A8):

$$0 = \int_0^{\infty} d\varepsilon\ \nu_d(\varepsilon) \left[\frac{\tanh(\frac{1}{2}\beta\eta_{\varepsilon})}{\eta_{\varepsilon}} - \frac{\tanh(\frac{1}{2}\beta_c\varepsilon)}{\varepsilon}\right]\ . \tag{A10}$$

Note that $[\cdots] \sim 1/\varepsilon^3$ for $\varepsilon \gg \max\{\beta^{-1}, \beta_c^{-1}, U\Delta\} \simeq \beta_c^{-1}$. As a consequence the energy integration is effectively restricted to $\varepsilon = O(\beta_c^{-1})$, so that $\nu_d(\varepsilon)$ can be replaced by $\nu_d(0)$. With the definitions $y \equiv \frac{1}{2}\beta_c\varepsilon$, $\delta \equiv \frac{1}{2}\beta_c\alpha U\Delta$, and $\theta \equiv T/T_c = \beta_c/\beta$, Eq. (A10) reduces to Eq. (7), which determines $\delta(\theta)$, and hence $\Delta(T)$, for $U \downarrow 0$.

To determine the precise value of $\Delta(T = 0)$, we set $\theta = 0$ in (7) and obtain an implicit equation for $\delta(\theta = 0) \equiv \delta_0$:

$$0 = \int_0^{\infty} dy \left[\frac{1}{\sqrt{y^2 + \delta_0^2}} - \frac{\tanh y}{y}\right]\ . \tag{A11}$$

The value of δ_0 can be calculated explicitly by multiplying $[\cdots]$ with an exponential factor $e^{-\kappa y}$, calculating both terms in (A11) separately and taking the limit $\kappa \downarrow 0$ in the end. The separate integrals can be expressed in terms of gamma functions, Weber's function $E_0(z)$ and von Neumann's function $N_0(z)$ for $z = \kappa\delta$. Details can be found in Ref. 53, formula (3.395.3), (3.551.9), (8.403.2), and (8.581.2). One finds as the result that the right hand side of (A11) is equal to $\ln(\pi/2\delta_0) - \gamma$, where $\gamma \simeq 0.577$ is Euler's constant. As a consequence,

$$\delta_0 = \tfrac{1}{2}\pi e^{-\gamma}, \qquad \Delta(T = 0) = \frac{\pi e^{-\gamma}}{\alpha U \beta_c}\ . \tag{A12}$$

It is also possible to calculate $\Delta(T)$ at low temperatures $T > 0$, such that $\theta = T/T_c \ll 1$. As the result one finds that the correction terms to (A12) are exponentially small for small θ:

$$\delta(\theta) \sim \delta_0 \left[1 - \sqrt{\frac{\theta\pi}{\delta_0}} e^{-2\delta_0/\theta}\right] \qquad (\theta \downarrow 0)\ . \tag{A13}$$

On the other hand, near T_c Eq. (7) predicts mean field critical behavior for the order parameter,

$$\delta(\theta) \sim \sqrt{(1-\theta)/Z}\ , \tag{A14}$$

where Z is defined by

$$Z \equiv \int_0^{\infty} dz \left[\frac{\sinh(2z) - 2z}{4z^3 \cosh^2(z)}\right]\ .$$

The numerical value of Z is $\simeq 0.426$. Results for $\Delta(T)$ are obtained from the relation $\Delta(T) = 2\delta(\theta)/\alpha U\beta_c$. Thus, $\Delta(T) \propto (T_c - T)^{1/2}$, as usual in a mean field treatment.

Next we calculate the free energy gain (per site) due to symmetry breaking. The free energy gain follows from the expression for the grand potential as

$$\begin{aligned}\Omega_S^H &\equiv \omega(T,\Delta) - \omega(T,\Delta = 0) \qquad\qquad (A15)\\ &= \tfrac{1}{2}\alpha U\Delta^2 - \frac{4}{\beta}\int_0^{\infty} d\varepsilon\ \nu_d(\varepsilon) \ln\left[\frac{\cosh(\frac{1}{2}\beta\eta_{\varepsilon})}{\cosh(\frac{1}{2}\beta\varepsilon)}\right]\\ &= \tfrac{1}{2}\alpha U\Delta^2 \left\{1 - 2\alpha U \frac{2\theta}{\delta^2}\int_0^{\infty} dy\ \nu_d(2y/\beta_c) \times \ln\left[\frac{\cosh(\sqrt{y^2+\delta^2}/\theta)}{\cosh(y/\theta)}\right]\right\}\ .\end{aligned}$$

In the last step, we used the dimensionless variables introduced above (7). If one inserts into (A15) the T_c criterion in the form

$$1 = 2\alpha U \int_0^{\infty} dy\ \nu_d(2y/\beta_c) \frac{\tanh(y)}{y}\ ,$$

one obtains the expression

$$\Omega_S^H = -\alpha^2 U^2 \Delta^2 \int_0^{\infty} dy\ \nu_d\left(\frac{2y}{\beta_c}\right) \times \left\{\frac{2\theta}{\delta^2} \ln\left[\frac{\cosh(\sqrt{y^2+\delta^2}/\theta)}{\cosh(y/\theta)}\right] - \frac{\tanh(y)}{y}\right\}\ ,$$

which is still exact. The integration is again effectively restricted to y values of order unity, so that in the limit $U \downarrow 0$, or $\beta_c \to \infty$, the factor $\nu_d(2y/\beta_c)$ can be replaced by $\nu_d(0)$. Consequently, one finds for small U that

$$\Omega_S^H \sim -\alpha^2 U^2 \Delta^2 \nu_d(0) \int_0^{\infty} dy \times \left\{\frac{2\theta}{\delta^2} \ln\left[\frac{\cosh(\sqrt{y^2+\delta^2}/\theta)}{\cosh(y/\theta)}\right] - \frac{\tanh(y)}{y}\right\}\ . \tag{A16}$$

The integral in the right hand side is convergent for all values of θ; it vanishes for $\theta \uparrow 1$ and approaches the value $\frac{1}{2}$ for $\theta \downarrow 0$.

APPENDIX B: PERTURBATION THEORY AT CONSTANT ORDER PARAMETER

In this appendix we extend the method of Ref. 39 to positive temperatures and to nearest-neighbor interaction. For the purposes of this paper, it is, furthermore, convenient to formulate the perturbation expansion in position space. We will treat the SDW phase and the CDW phase simultaneously. In either phase, we consider a grand canonical Hamiltonian of the form

$$K = H_t + H_U + H_V + \mu(U)\left[N - \sum_{\mathbf{i}\sigma} n_{\mathbf{i}\sigma}\right] + h(U)\left[\mathcal{N}\Delta - \sum_{\mathbf{i}}(-1)^{\mathbf{i}} O_{\mathbf{i}}\right] , \tag{B1}$$

where either $O_{\mathbf{i}} = S^z_{\mathbf{i}} = n_{\mathbf{i}\uparrow} - n_{\mathbf{i}\downarrow}$ (SDW phase) or $O_{\mathbf{i}} = n_{\mathbf{i}} = n_{\mathbf{i}\uparrow} + n_{\mathbf{i}\downarrow}$ (CDW phase). The parameter $v \equiv V/U > 0$ is kept fixed in taking the limit $U \to 0$. The field $h(U)$ has been introduced to keep the staggered magnetization per site (SDW phase) or the staggered density per site (CDW phase) at a fixed value $\Delta > 0$. We focus on the special case of half filling ($N = \mathcal{N}$), so that the chemical potential is exactly given by $\mu(U) = (\frac{1}{2} + 2v)U$.

To formulate a perturbation expansion at fixed Δ we set $h(U) \equiv h_0(\Delta) + h_1(\Delta)U + \cdots$ for $U \to 0$, and we split off the U-independent terms in (B1) from the rest: $K = K_0 + K_1$, where K_1 is treated as a perturbation and

$$K_0 = H_t + h_0\left[\mathcal{N}\Delta - \sum_{\mathbf{i}}(-1)^{\mathbf{i}} O_{\mathbf{i}}\right] = H_t - \sum_{\sigma,\lambda} h_\sigma \lambda N^\lambda_\sigma + h_0 \mathcal{N}\Delta . \tag{B2}$$

Here, σ takes the values $(\uparrow,\downarrow)$ or alternatively $(+,-)$, and $\lambda = +$ on even sites and $\lambda = -$ on odd sites. In the second step we defined $h_\sigma \equiv r_\sigma h_0$, with $r_\sigma = \sigma$ for the SDW phase and $r_\sigma = 1$ for the CDW phase. Comparison with (A1) shows that h_σ plays the same role in (B2) as it played in Sec. A 1. As a consequence K_0 can be diagonalized in terms of new particles $d_{\mathbf{k}\sigma}, d^\dagger_{\mathbf{k}\sigma}$ with eigenenergies $\eta_{\mathbf{k}\sigma} = \mathrm{sgn}(\varepsilon_{\mathbf{k}})\sqrt{\varepsilon^2_{\mathbf{k}} + h_0^2}$. Many results now follow immediately. The consistency relation between the sublattice magnetization and the field h_0 is

$$\Delta = 2h_0 \int_0^\infty d\varepsilon\, \nu_d(\varepsilon) \frac{\tanh(\frac{1}{2}\beta\eta_\varepsilon)}{\eta_\varepsilon} \tag{B3}$$

and the free energy per site f_0 is given in (10a). Moreover, the Green functions corresponding to K_0 are simply given by the Hartree Green functions discussed in Appendix A 2.

The perturbation expansion of the free energy in powers of K_1 is

$$f - f_0 = \frac{1}{\beta\mathcal{N}} \int_0^\beta d\tau \langle K_1(\tau)\rangle^c_0 - \frac{1}{2\beta\mathcal{N}} \int_0^\beta \int_0^\beta d\tau_1 d\tau_2 \langle K_1(\tau_1) K_1(\tau_2)\rangle^c_0 + \cdots .$$

To calculate the various terms in this expansion we need $\mu(U)$ and $h(U)$ up to linear order in U. From the Maxwell relations[39] one finds that $(\partial\mu/\partial U)_{U=0} = (\frac{1}{2}+2v)$, so that $\mu \sim \frac{1}{2}U + 2V$ as expected, and

$$\left(\frac{\partial h}{\partial U}\right)_{U=0} = -(\alpha + C_d)\Delta ,$$

where

$$C_d \equiv 2v \frac{\partial}{\partial \Delta^2}\left([G_1(0)]^2\right)_{U=0} .$$

To obtain C_d correct to $O(d^{-1})$ it suffices to calculate $G_1(0)$ to $O(d^{-1/2})$. One then finds from the expression (A5) for $G^\lambda_\ell(\tau)$ with $\ell = 1$ that the derivative $\frac{\partial}{\partial\Delta^2}[G_1(0)]^2$ is of $O(U/d)$ for small U, so that $C_d = 0$ and, consequently, $h_1(\Delta) = -\alpha\Delta$.

With these values for μ and h_1 one can write the perturbation K_1 as

$$K_1 = \tilde{H}_U + \tilde{H}_V + \left(\frac{U}{4} + V\right)\mathcal{N} - \tfrac{1}{2}\alpha U \mathcal{N}\Delta^2 - 2\mathcal{N}V[G_1(0)]^2 ,$$
$$\tilde{H}_U = U\sum_{\mathbf{i}} \delta n_{\mathbf{i}\uparrow}\delta n_{\mathbf{i}\downarrow} \; ; \; \tilde{H}_V = \frac{V}{d}\sum_{\langle \mathbf{i},\mathbf{j}\rangle} \delta n_{\mathbf{i}}\delta n_{\mathbf{j}} , \tag{B4}$$

where we defined $\delta n_{\mathbf{i}\sigma} \equiv n_{\mathbf{i}\sigma} - \langle n_{\mathbf{i}\sigma}\rangle$ and $\delta n_{\mathbf{i}} \equiv \delta n_{\mathbf{i}\uparrow} + \delta n_{\mathbf{i}\downarrow}$. The expressions for f_1 and f_2, given in (10b) and (10c), respectively, follow automatically.

Finally, we show that, to linear order in U, the perturbation expansion of Ref. 39 leads to the Hartree (not the Hartree-Fock) approximation. From Eqs. (10a) and (B4) we find that, to linear order in U, the free energy per site is given by

$$f = f_0 + f_1 = h_0\Delta - \frac{4}{\beta}\int_0^\infty d\varepsilon\, \nu_d(\varepsilon) \ln\left[2\cosh\left(\tfrac{1}{2}\beta\eta_\varepsilon\right)\right] + \left(\frac{U}{4} + V\right) - \tfrac{1}{2}\alpha U\Delta^2 - 2V[G_1(0)]^2 . \tag{B5}$$

The free energy is minimal if

$$0 = \frac{\partial f}{\partial h_0} \sim (h_0 - \alpha U\Delta)\frac{\partial\Delta}{\partial h_0} , \tag{B6}$$

so that h_0 and Δ are related by $h_0 \sim \alpha U\Delta$, which is precisely the same condition as was previously found from the Hartree approximation in Appendix A. In the derivation of (B6) we used the consistency condition (B3). Note that the Fock term [last term in (B5)] does not contribute to (B6) to dominant order: this term leads to a negligibly small correction, of relative order U/d. Thus, the Fock term is of the same order as the second-order contributions (10c). Hence it has to be taken into account in the calculation of the free energy to order U^2.

APPENDIX C: CALCULATION OF DIAGRAMS (a), (b), AND (f)

In this appendix, we summarize the most important steps in the calculation of the Fock diagram (a), the

second-order U^2 diagram (b), and the third-order U^3 diagram (f).

1. Diagram (a)

The calculation of diagram (a) has been reduced to that of B_a in (15). In order to calculate $B_a(h_0,\beta)$, we split up the factor JJ' into various parts:

$$\begin{aligned} J(h_0^2,\beta)J'(h_0^2,\beta) &= J(0,\beta_c)J'(0,\beta_c) \\ &+ \left[J(h_0^2,\beta)-J(0,\beta_c)\right]J'(0,\beta_c) \\ &+ J(h_0^2,\beta)\left[J'(h_0^2,\beta)-J'(0,\beta_c)\right] . \end{aligned} \tag{C1}$$

The first line represents JJ' at T_c; the temperature dependence of B_a is contained in the last two lines. The first line in (C1) can be calculated in an elementary way: the J factor reduces to an integral over $\nu_\infty(\varepsilon)$, and the J' integral has a logarithmic divergence which is cut off at $\varepsilon \simeq \beta_c^{-1}$. The result is $-1/(4\sqrt{2\pi\alpha U})$ for $U \to 0$. The second line in (C1) leads to a result which is negligible, of relative order T_c^2, compared to the first line. In order to analyze the third line we transform from ε to the rescaled energy $y \equiv \frac{1}{2}\beta_c\varepsilon$ and similarly from h_0 to $\delta \equiv \frac{1}{2}\beta_c h_0$ and from T to $\theta \equiv T/T_c$. The dominant contribution comes from small energies, $\varepsilon = O(\beta_c^{-1})$, which corresponds to $y = O(1)$. In the limit $U \to 0$, or $\beta_c \to \infty$ [see below (13)] the third line reduces to a function $\Psi_a(\delta,\theta)$ depending only on the rescaled variables δ and θ. Since $\Psi_a(\delta,\theta) = O(1)$ for $U \downarrow 0$, we conclude that the third line is smaller than the first line by a factor of U, so that it can also be neglected. Thus, we obtain the result given in Eq. (16) in Sec. IV.

2. Diagram (b)

To calculate diagram (b) we consider the integral $\mathcal{I}_b(\beta)$ in (18). According to Appendix A 2 the Green function $G_0(\tau)$ has the form

$$G_0(\tau) = P(\tau;\beta,h_0^2) - h_0 Q(\tau;\beta,h_0^2) , \tag{C2}$$

where

$$P(\tau;\beta,h_0^2) = \mathrm{sgn}(\tau)\int_0^\infty d\varepsilon\ \nu_d(\varepsilon)\frac{\cosh\left[\left(\frac{1}{2}\beta-|\tau|\right)\eta_\varepsilon\right]}{\cosh\left[\frac{1}{2}\beta\eta_\varepsilon\right]} ,$$

$$Q(\tau;\beta,h_0^2) = \int_0^\infty d\varepsilon\ \nu_d(\varepsilon)\frac{\sinh\left[\left(\frac{1}{2}\beta-|\tau|\right)\eta_\varepsilon\right]}{\eta_\varepsilon\cosh\left[\frac{1}{2}\beta\eta_\varepsilon\right]} .$$

As a consequence the integral $\mathcal{I}_b(\beta)$ in (18) takes the form

$$\mathcal{I}_b(\beta) = \int_0^\beta d\tau\left[P^2(\tau;\beta,h_0^2) - h_0^2 Q^2(\tau;\beta,h_0^2)\right]^2 . \tag{C3}$$

Again we do not need the free energy f_b itself but only its derivative $B_b(h_0,\beta)$. Hence, we need only

$$\begin{aligned} \mathcal{J}_b(h_0,\beta) &\equiv \frac{1}{h_0}\frac{\partial\mathcal{I}_b}{\partial h_0} \\ &= 8\int_0^{\beta/2} d\tau\ K(\tau;\beta,h_0^2)K'(\tau;\beta,h_0^2) , \end{aligned} \tag{C4}$$

where we defined $K \equiv P^2 - h_0^2Q^2$ and $K' \equiv \partial K/\partial h_0^2$. Note that the domain of integration can be restricted to $0 < \tau < \beta/2$ since $K(\tau;\beta,h_0^2)$ is symmetric under $\tau \to \beta - \tau$. Below we will evaluate $\mathcal{J}_b(h_0,\beta)$, first for $T = T_c$ and then for $T < T_c$.

At T_c, Eq. (C4) simplifies drastically, since the factor K in the right hand side reduces to $P^2(\tau;\beta_c,0)$ and

$$K'(\tau;\beta_c,0) = P(\tau;\beta_c,0)\Xi(\tau;\beta_c) - Q^2(\tau;\beta_c,0) ,$$

where $\Xi(\tau;\beta)$ is defined as

$$\Xi(\tau;\beta) \equiv \int_0^\infty d\varepsilon\ \nu_d(\varepsilon)\left\{\frac{\left(\frac{1}{2}\beta-\tau\right)\sinh\left[\left(\frac{1}{2}\beta-\tau\right)\varepsilon\right]}{\varepsilon\cosh\left(\frac{1}{2}\beta\varepsilon\right)} - \frac{\frac{1}{2}\beta\tanh\left(\frac{1}{2}\beta\varepsilon\right)\cosh\left[\left(\frac{1}{2}\beta-\tau\right)\varepsilon\right]}{\varepsilon\cosh\left(\frac{1}{2}\beta\varepsilon\right)}\right\} .$$

For $U \to 0$, or $\beta_c \to \infty$ [see (13)], one has

$$P(\tau;\beta_c,0) \sim \int_0^\infty d\varepsilon\ \nu_d(\varepsilon)e^{-\varepsilon\tau} \equiv \hat{\nu}_d(\tau) , \tag{C5a}$$

$$\Xi(\tau;\beta_c) \sim -\tau\nu_d(0)\ln(\beta_c) \sim -\frac{\tau}{2\alpha U} , \tag{C5b}$$

$$Q(\tau;\beta_c,0) \sim \nu_d(0)\ln(\beta_c) \sim \frac{1}{2\alpha U} . \tag{C5c}$$

Insertion of these results into (C4) gives

$$\begin{aligned} \mathcal{J}_b(0,\beta_c) &\sim -8\int_0^{\beta_c/2} d\tau\left\{\frac{\tau}{2\alpha U}\left[\hat{\nu}_d(\tau)\right]^3 + \frac{1}{4\alpha^2U^2}\left[\hat{\nu}_d(\tau)\right]^2\right\} \\ &\sim -\frac{2}{\alpha^2U^2}\int_0^\infty d\tau\ \left[\hat{\nu}_d(\tau)\right]^2 \qquad (U \to 0) , \end{aligned} \tag{C6}$$

and hence

$$B_b(0,\beta_c) \sim \gamma_d/\alpha^2 \qquad (U \to 0)\ ;\ \gamma_d \equiv \int_0^\infty d\tau\ \left[\hat{\nu}_d(\tau)\right]^2 .$$

The problem of calculating $B_b(0,\beta_c)$ has thus been reduced to the calculation of γ_d. In high dimensions, it is not difficult to calculate γ_d explicitly up to $O(d^{-1})$, using the density of states (A9). The result is

$$\gamma_d = \gamma_\infty - \tfrac{3}{32d}\left(\gamma_\infty + \tfrac{1}{3\sqrt{2\pi}}\right) + O(d^{-2}) , \tag{C7}$$

where $\gamma_\infty \equiv \frac{1}{2\sqrt{\pi}}\ln\tan(3\pi/8)$, which can, if desired, be rewritten as $\gamma_\infty = \frac{1}{2\sqrt{\pi}}\ln(\sqrt{2}+1)$.

Next we address the calculation of the integral $\mathcal{J}_b(h_0,\beta)$ in (C4) for $T < T_c$. For this purpose, we consider the difference of $\mathcal{J}_b(h_0,\beta)$ and its value $\mathcal{J}_b(0,\beta_c)$ at T_c, which can conveniently be split up as follows:

$$\mathcal{J}_b(h_0,\beta)-\mathcal{J}_b(0,\beta_c)=8\int_0^{\beta_c/2}d\tau\ K(\tau;\beta,h_0^2)\left[K'(\tau;\beta,h_0^2)-K'(\tau;\beta_c,0)\right]$$
$$+8\int_0^{\beta_c/2}d\tau\ \left[K(\tau;\beta,h_0^2)-K(\tau;\beta_c,0)\right]K'(\tau;\beta_c,0)$$
$$+8\int_{\beta_c/2}^{\beta/2}d\tau\ K(\tau;\beta,h_0^2)K'(\tau;\beta,h_0^2)\ . \tag{C8}$$

The calculation of the various terms in (C8) is rather lengthy, but the result is simple. Both the second and the third line on the right in (C8) are exponentially small compared to $\mathcal{J}_b(0,\beta_c)$, of relative order k_BT_c. Hence these terms can be neglected. Moreover, the first line in (C8), too, is small compared to $\mathcal{J}_b(0,\beta_c)$, but now of relative order U. Thus, one finds that the asymptotic behavior of $\mathcal{J}_b(h_0,\beta)$ for $U\downarrow 0$ is *independent* of temperature for all $T<T_c$:

$$B_b(h_0,\beta)\sim B_b(0,\beta_c)$$
$$\sim\gamma_d/\alpha^2\qquad(U\to 0)\ ,$$

which is precisely the result given in Eq. (19) in the main text.

3. Diagram (f)

In order to calculate the free energy contribution f_f due to diagram (f), we note that $T(\tau_1,\tau_2,\tau_3)$ in (24) is symmetric in the time indices τ_i $(i=1,2,3)$. Hence, f_f in (24) is equal to $6\times$ the integral over the region $\tau_3>\tau_2>\tau_1$. It is, furthermore, convenient to transform from (τ_1,τ_2) to variables (τ_{31},τ_{21}), yielding

$$f_f=\frac{U^3r_\downarrow}{\beta}\int_0^\beta d\tau_3\int_0^{\tau_3}d\tau_{31}\int_0^{\tau_{31}}d\tau_{21}\ [T(\tau_1,\tau_2,\tau_3)]^2\ . \tag{C9}$$

The rationale behind this transformation is that $T(\tau_1,\tau_2,\tau_3)$ is a function only of (τ_{31},τ_{21}) and that the dominant contribution to the integral in (C9) comes from (τ_1,τ_2,τ_3) values which are close together, so that τ_{31} and τ_{21} are of order unity. To calculate the right hand side of (C9), we introduce the shorthand notation $P_{nm}\equiv P(\tau_{nm};\beta_c,0)$ and similarly $Q_{nm}\equiv Q(\tau_{nm};\beta_c,0)$, with P and Q defined below (C2). In this notation

$$T(\tau_1,\tau_2,\tau_3)=-2h_0(Q_{21}P_{32}P_{13}$$
$$+P_{21}Q_{32}P_{13}+P_{21}P_{32}Q_{13})+O(h_0^3)\ .$$

Note that $T(\tau_1,\tau_2,\tau_3)$ is exponentially small, of order h_0. From (C5) we know that for $U\downarrow 0$, or $\beta_c\to\infty$, P_{nm} remains finite: $P_{nm}\sim\mathrm{sgn}(\tau_{nm})\hat{\nu}_d(\tau_{nm})$; whereas Q_{nm} becomes large: $Q_{nm}\sim(2\alpha U)^{-1}$. This gives

$$T(\tau_1,\tau_2,\tau_3)\sim-\frac{h_0}{\alpha U}\left(P_{32}P_{13}+P_{21}P_{13}+P_{21}P_{32}\right)\ .$$

Insertion into (C9) finally gives a very simple result for the free energy contribution due to diagram (f), namely, $f_f=\frac{1}{2}Ur_\downarrow\bar{C}_fh_0^2$, where the (positive) constant $\bar{C}_f$ is defined as

$$\bar{C}_f=2\alpha^{-2}\int_0^\infty dt_1\int_0^{t_1}dt_2\ [\hat{\nu}_d(t_2)\hat{\nu}_d(t_1-t_2)$$
$$-\hat{\nu}_d(t_1-t_2)\hat{\nu}_d(t_1)-\hat{\nu}_d(t_2)\hat{\nu}_d(t_1)]^2\ .$$

It is easy to show that the integral on the right is finite.

APPENDIX D: SUMMARY OF RESULTS FOR SPINLESS FERMIONS

The Hamiltonian for spinless fermions is given by

$$H^{\mathrm{SF}}=-\frac{t}{\sqrt{2d}}\sum_{\langle\mathbf{ij}\rangle}(c_\mathbf{i}^\dagger c_\mathbf{j}+\mathrm{H.c.})+\frac{V}{d}\sum_{\langle\mathbf{ij}\rangle}n_\mathbf{i}n_\mathbf{j}\ . \tag{D1}$$

The spinless fermion model is closely related to the extended Hubbard model at $U=0$, which is the natural generalization of H^{SF} to two colors (spin species). The similarity becomes clear already at Hartree level. If we denote the Hartree critical temperature, order parameter and free energy for spinless fermions (1 color) by $T_c^{(H1)}$, $\Delta^{(H1)}$, and $f^{(H1)}$ and those in the extended Hubbard model at $U=0$ (2 colors) by $T_c^{(H2)}$, $\Delta^{(H2)}$, and $f^{(H2)}$, then

$$T_c^{(H1)}(V)=T_c^{(H2)}(\tfrac{1}{2}V)\ ,$$
$$\Delta^{(H1)}(V,T)=\Delta^{(H2)}(\tfrac{1}{2}V,T)\ ,$$
$$f^{(H1)}(V,T)=\tfrac{1}{2}f^{(H2)}(\tfrac{1}{2}V,T)\ .$$

Clearly the tendency towards symmetry breaking is smaller (i.e., the fluctuations are larger) for spinless fermions than for the model with two colors.

The calculations in second-order perturbation theory are very similar to those for the extended Hubbard model. The only diagrams that yield nonvanishing corrections to the Hartree approximation as $V\downarrow 0$ are the Fock diagram (a) and diagram (d) in Fig. 2. One finds that, for $V\downarrow 0$, the derivatives $B_a^{(1)}(h_0,\beta)$ and $B_d^{(1)}(h_0,\beta)$ of the corresponding free energy contributions are *identical* to the values calculated for the extended Hubbard model in Sec. IV:

$$B_a^{(1)}(h_0,\beta)+B_d^{(1)}(h_0,\beta)=\frac{1}{2d\sqrt{2\pi}}+\frac{\gamma_\infty}{d}\equiv\bar{C}^{(1)}\ ,$$

where γ_∞ is defined in (C7). The value of h_0 is determined by the condition that the free energy be minimal:

$$0 = \frac{d}{d\Delta}\left(f^{(H1)} + f_a^{(1)} + f_d^{(1)}\right)$$

$$= \tfrac{1}{2}\left(h_0 - V\Delta\right) + \bar{C}^{(1)} h_0 \frac{dh_0}{d\Delta} \ .$$

Since $dh_0/d\Delta \sim V$ for $V \downarrow 0$, it follows that the actual critical temperature and order parameter for spinless fermions are obtained from the Hartree expressions by replacing V with $V/(1 + 2V\bar{C}^{(1)})$. This implies that the q factor for spinless fermions, defined by

$$T_c^{(1)} = q^{\mathrm{SF}} T_c^{(H1)}; \qquad \Delta^{(1)}(T) = q^{\mathrm{SF}} \Delta^{(H1)}(T/q^{\mathrm{SF}})$$

is for $V \downarrow 0$ given by

$$q^{\mathrm{SF}} = e^{-\bar{C}^{(1)}/\nu_\infty(0)} = e^{-C_1' d^{-1}} \ ,$$

$$C_1' = \tfrac{1}{2} + \tfrac{1}{2}\sqrt{2}\ln\left[\tan\left(\tfrac{3\pi}{8}\right)\right] \ . \qquad \text{(D2)}$$

Note that the numerical value of C_1' is twice that of the corresponding constant C_1 for the extended Hubbard model with $U = 0$, see (30).

[1] J. W. Negele and H. Orland, *Quantum Many-Particle Systems* (Addison-Wesley, New York, 1987); A. L. Fetter and J. D. Walecka, *Quantum Theory of Many-Particle Systems* (McGraw-Hill, New York, 1971).

[2] J. Goldstone, Proc. R. Soc. London Ser. A **239**, 267 (1957).

[3] W. Langer, M. Plischke, and D. Mattis, Phys. Rev. Lett. **23**, 1448 (1969).

[4] J. Bardeen, L. N. Cooper, and J. R. Schrieffer, Phys. Rev. **108**, 1175 (1957).

[5] N. D. Mermin and H. Wagner, Phys. Rev. Lett. **17**, 1133 (1966); P. C. Hohenberg, Phys. Rev. **158**, 383 (1967).

[6] P. G. J. van Dongen, Phys. Rev. Lett. **67**, 757 (1991).

[7] J. Hubbard, Proc. R. Soc. London Ser. A **276**, 238 (1963); M. C. Gutzwiller, Phys. Rev. Lett. **10**, 59 (1963); J. Kanamori, Prog. Theor. Phys. **30**, 275 (1963).

[8] N. F. Mott, Rev. Mod. Phys. **40**, 677 (1968); W. F. Brinkman and T. M. Rice, Phys. Rev. B **2**, 4302 (1970).

[9] P. W. Anderson, Solid State Phys. **14**, 99 (1963).

[10] M. Cyrot, Physica **91B**, 141 (1977); for a recent numerical study of the paramagnetic small-U Hubbard model, see H. Schweitzer and G. Czycholl, Z. Phys. B **83**, 93 (1991).

[11] Y. Nagaoka, Phys. Rev. **147**, 392 (1966); H. Tasaki, Phys. Rev. B **40**, 9192 (1989).

[12] H. J. Schulz, Phys. Rev. Lett. **64**, 1445 (1990).

[13] P. W. Anderson, Science **235**, 1196 (1987).

[14] P. A. Lee and N. Nagaosa, Phys. Rev. B **46**, 5621 (1992).

[15] W. Metzner and D. Vollhardt, Phys. Rev. Lett. **62**, 324 (1989).

[16] E. Müller-Hartmann, Z. Phys. B **74**, 507 (1989).

[17] J. Solyom, Adv. Phys. **21**, 201 (1979); V. J. Emery, in *Highly Conducting One-Dimensional Solids*, edited by J. Devreese, R. Evrand, and V. van Doren (Plenum, New York, 1979).

[18] R. A. Bari, Phys. Rev. B **3**, 2662 (1971).

[19] P. G. J. van Dongen, Phys. Rev. B **49**, 7904 (1994).

[20] J. E. Hirsch, Phys. Rev. Lett. **53**, 2327 (1984).

[21] D. K. Campbell, J. Tinka Gammel, and E. Y. Loh, Jr., Phys. Rev. B **42**, 475 (1990).

[22] F. Mila and X. Zotos, Europhys. Lett. **24**, 133 (1993); K. Penc and F. Mila, Phys. Rev. B **49**, 9670 (1994).

[23] U. Wolff, Nucl. Phys. B **225**, 391 (1983).

[24] R. Brout, Phys. Rev. **118**, 1009 (1960); C. J. Thompson, Commun. Math. Phys. **36**, 255 (1974).

[25] P. A. Pearce and C. J. Thompson, Commun. Math. Phys. **58**, 131 (1978); T. Kennedy, E. H. Lieb, and B. S. Shastry, Phys. Rev. Lett. **61**, 2582 (1988); J. Stat. Phys. **53**, 1019 (1988).

[26] For reviews, see, D. Vollhardt, Int. J. Mod. Phys. B **3**, 2189 (1989); E. Müller-Hartmann, *ibid.* **3**, 2169 (1989).

[27] U. Brandt and C. Mielsch, Z. Phys. B **75**, 365 (1989); **79**, 295 (1990).

[28] P. G. J. van Dongen and D. Vollhardt, Phys. Rev. Lett. **65**, 1663 (1990).

[29] P. G. J. van Dongen, Phys. Rev. B **45**, 2267 (1992).

[30] V. Janiš, Z. Phys. B **83**, 227 (1991).

[31] A. Georges and G. Kotliar, Phys. Rev. B **45**, 6479 (1992).

[32] M. Jarrell, Phys. Rev. Lett. **69**, 168 (1992).

[33] M. Jarrell and Th. Pruschke, Z. Phys. B **90**, 187 (1993).

[34] M. J. Rozenberg, X. Y. Zhang, and G. Kotliar, Phys. Rev. Lett. **69**, 1236 (1992).

[35] A. Georges and W. Krauth, Phys. Rev. Lett. **69**, 1240 (1992); Phys. Rev. B **48**, 7167 (1993).

[36] This excludes, e.g., ferromagnetic and ferrimagnetic solutions. The justification is that such solutions are unstable in Hartree approximation (i.e., at weak coupling). The validity of (3), at least within Hartree-Fock theory, has recently been proved for the Hubbard model ($v = 0$) by V. Bach, E. H. Lieb, and J. Ph. Solovej (unpublished).

[37] Following a suggestion by Müller-Hartmann, I investigated the possibility of phases with a mixed SDW-CDW character, which have $r_\uparrow = 1$ and $|r_\downarrow| \neq 1$. It turns out that these phases have a higher Hartree free energy than the pure SDW or CDW states, so that they, too, can be excluded from consideration.

[38] See, e.g., N. W. Ashcroft and N. D. Mermin, *Solid State Physics* (Holt-Saunders, Tokyo, 1976), Chap. 34.

[39] A. Georges and J. S. Yedidia, Phys. Rev. B **43**, 3475 (1991).

[40] N. E. Bickers and D. J. Scalapino, Ann. Phys. **193**, 206 (1989); N. E. Bickers and S. R. White, Phys. Rev. B **43**, 8044 (1991).

[41] G. Baym and L. P. Kadanoff, Phys. Rev. **124**, 287 (1961); G. Baym, *ibid.* **127**, 1391 (1962).

[42] This restriction is for convenience only. It could be released, if desired, but this would imply that one has to drag along factors like $U \ln\beta_c$ and $U \ln h_0(T = 0)$, which would make the calculations messier and less transparent. Here I have anticipated that, in the end, these quantities are both of order unity.

[43] The results of the $1/d$ expansions may be relevant to $d \geq 3$ only. There are arguments by P. Kopietz, Phys. Rev. B **48**, 13 789 (1993), suggesting that the method of Georges and Yedidia (Ref. 39) is not systematic in $d = 1, 2$.

[44] In fact there exist also simulations of the Hubbard model in $d = 3$, e.g., by R. T. Scalettar, D. J. Scalapino, R. L. Sugar, and D. Toussaint, Phys. Rev. B **39**, 4711 (1989), but I suspect that the critical temperatures found there are too high. As discussed also in Ref. 33, the critical temperatures obtained by Scalettar *et al.* in $d = 3$ are even higher than

those in $d = \infty$. This contradicts the general tendency that $T_{\text{Néel}}$ increases with dimension.

[45] J. K. Freericks, Phys. Rev. B **50**, 403 (1994); J. K. Freericks, M. Jarrell, and D. J. Scalapino, Europhys. Lett. **25**, 37 (1994).

[46] For an excellent review of the negative-U Hubbard model, see R. Micnas, J. Ranninger, and S. Robaszkiewicz, Rev. Mod. Phys. **62**, 113 (1990).

[47] V. J. Emery, Phys. Rev. B **14**, 2989 (1976).

[48] A. Martín-Rodero and F. Flores, Phys. Rev. B **45**, 13 008 (1992).

[49] Y. Zhang and J. Callaway, Phys. Rev. B **39**, 9397 (1989).

[50] R. Shankar, Int. J. Mod. Phys. B **4**, 2371 (1990); Physica A **177**, 530 (1991); Rev. Mod. Phys. **66**, 129 (1994).

[51] G. S. Uhrig and R. Vlaming, Phys. Rev. Lett. **71**, 271 (1993); J. Phys. C **5**, 2561 (1993).

[52] E. Halvorsen, G. S. Uhrig, and G. Czycholl, Z. Phys. B **94**, 291 (1994).

[53] I. S. Gradshteyn and I. M. Ryzhik, *Table of Integrals, Series and Products* (Academic Press, New York, 1980).